Tasmanian Geological Survey
Record 2013/03

Geology of parts of the Bathurst and Maatsuyker map sheets

by P. G. Lennox

Mineral Resources Tasmania
Department of Infrastructure, Energy and Resources

Tasmania
Explore the possibilities

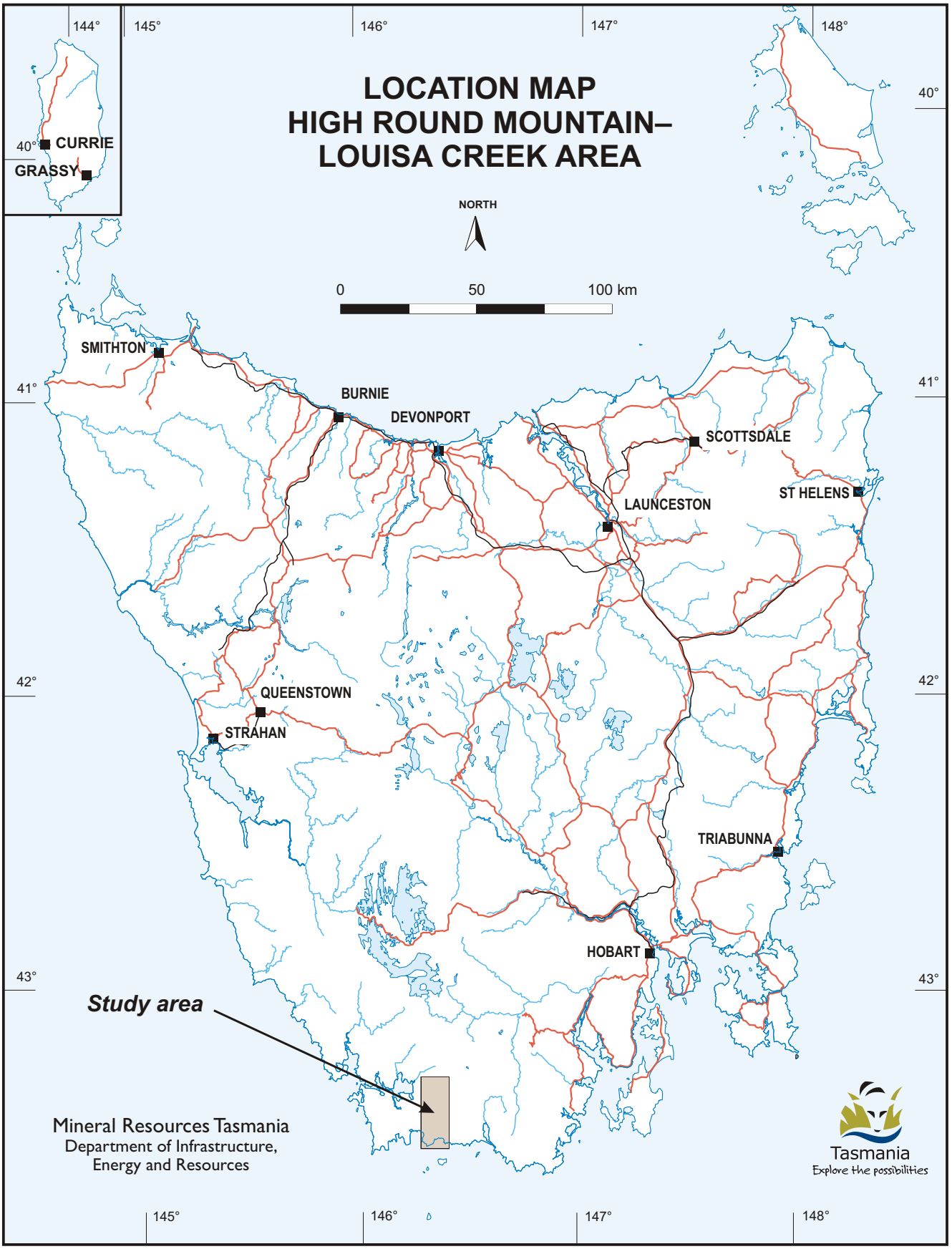

Mineral Resources Tasmania PO Box 56 Rosny Park Tasmania 7018
Phone: (03) 6233 8377 ● Fax: (03) 6233 8338
Email: info@mrt.tas.gov.au ● Internet: www.mrt.tas.gov.au

CONTENTS

PLATES

TABLES

FIGURES

Introduction

These notes were prepared by P. G. Lennox of Tasmania Department of Mines in 1980 following fieldwork undertaken in South West Tasmania. Mapping in the High Round Mountain area (443000/5201300), east of Bathurst Harbour, was undertaken during a twelve-day field trip in February 1980 (fig. 1). The area immediately to the north, including Harrys Bluff (442300/5205300), Junction Ridge (444000/5207200) and Ripple Mountain (443800/ 5209700) was mapped by P. R. Williams of Tasmania Department of Mines. The geology of the High Round Mountain to Lone Hill area forms part A of this report.

The Louisa Creek (446700/5185600) area was mapped by P. G. Lennox during a twelve-day field trip in late February–early March 1980. As shown in Figure 2 this area covers part of the Bathurst map sheet and the northeastern section of the Maatsuyker map sheet.

All grid references in the text are AGD66 datum and are MGA co-ordinates in Zone 55, quoted in the form xxxxxx/yyyyyyy, where the first six numbers are metres east and the last seven numbers are metres north.

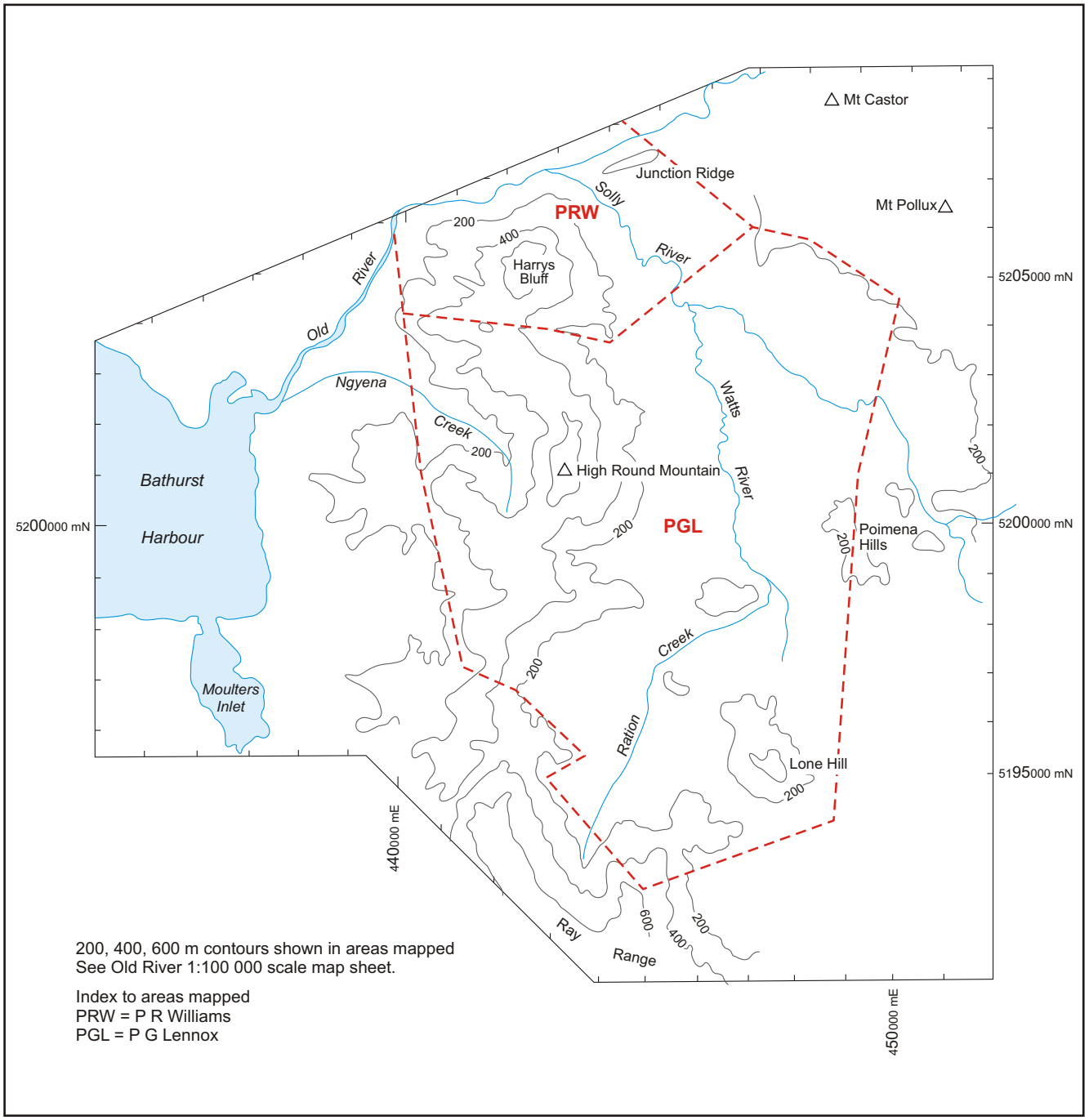

Figure 1

Locality map and mapping areas, High Round Mountain area

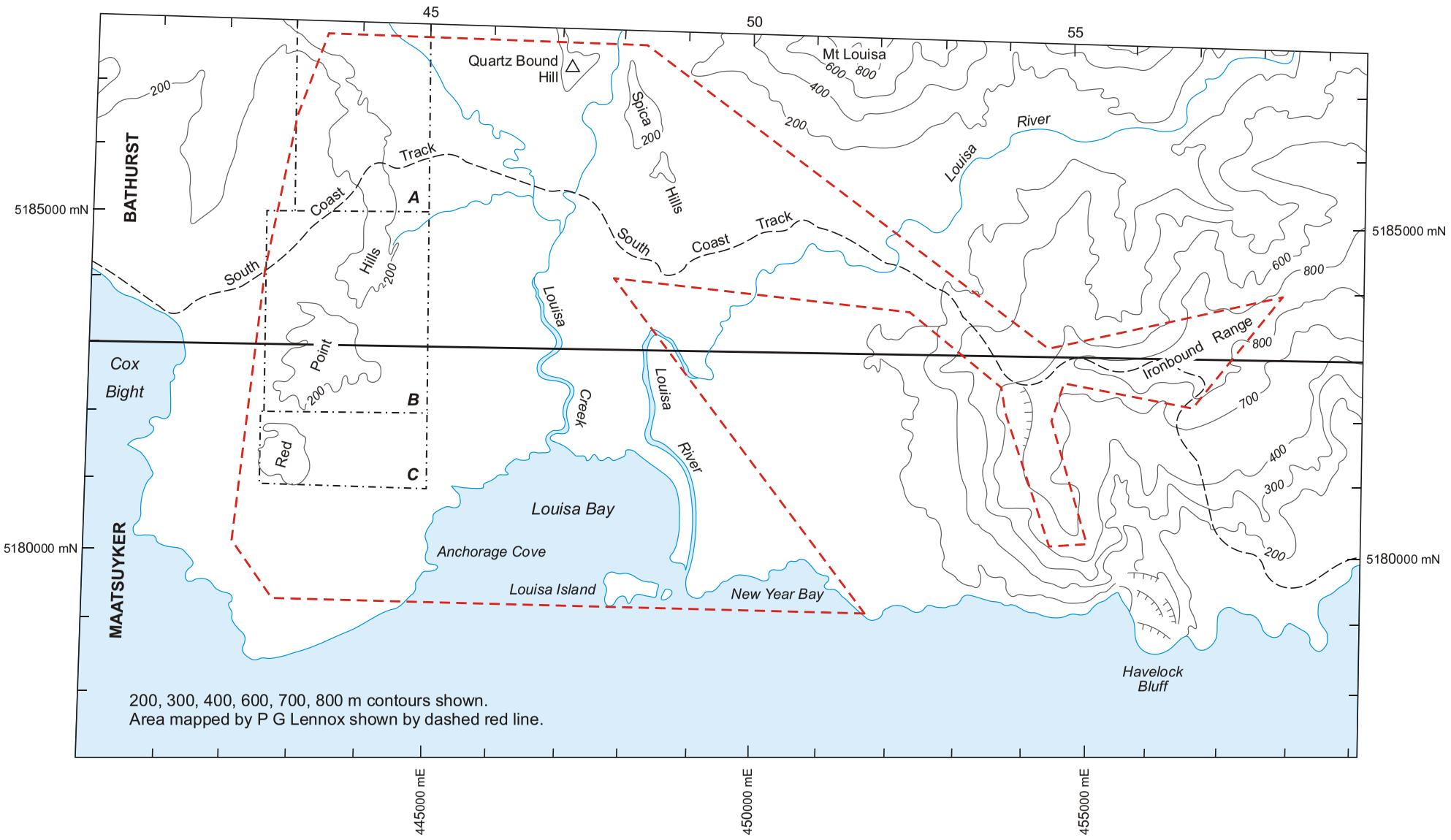

Sub-areas for structural mapping (fig. 19, 20) —
A = north of South Coast Track; B = between Ravine Creek and South Coast Track; C = south of Ravine Creek

Figure 2
Locality map and mapping areas, Louisa Creek area

Part A — High Round Mountain area

Introduction

This region includes High Round Mountain, Poimena Hills (448700/5200000), Ration Creek (445000/5197400), Lone Hill (447300/5195400) and parts of the Ray Range south of High Round Mountain (441500/5198000) and adjacent to Lone Hill (445600/5194400). Where accessible the Solly River and its tributary the Watts River were investigated.

Previous exploration in this area includes the work of Hall *et al.* (1969) for the Exploration Department of the Broken Hill Proprietary Company Ltd. Hall *et al.* (1969) refer to Precambrian rocks of chlorite grade and uncertain correlation in the Solly River area. They note that the Solly River area consists of a massive quartzite overlain by phyllite and pelitic quartz-chlorite schist with thin bands of green schist and stretched conglomerate and dark graphitic schists. These rocks have a simple structure and dip moderately steeply northwest.

On the basis of the work of Hall *et al.* (1969) the Port Davey 1:250 000 geological map (Williams and Corbett, 1977) showed the High Round Mountain area underlain entirely by Precambrian metaquartzite sequences.

Stratigraphy

The metamorphic rocks exposed in the High Round Mountain–Lone Hill area can be subdivided into three distinctive lithologies; quartzite, micaceous-quartzite and phyllite. The tectonic(?) surfaces identified in the field by P. R. Williams (pers. comm.) in the Harrys Bluff area are shown in Table 1. The mechanical layering (S_2), which is parallel to the bedding, has preserved on it a number of bedding structures (ripples and cross bedding). In the High Round Mountain area a number of outcrops show apparent cross bedding and ripples as shown in Figures 3 and 4. Table 2 is a list of all possible cross-bedded/cross-laminated outcrops and the few possible examples of outcrops containing ripple marks. In all cases shown in Table 2 the cross-bedding/cross-lamination indicates the sequence to be the right way up. In one outcrop at the eastern end of the Ray Range (444600/5195000) the quartzite exhibits possible grading.

Figure 5 shows a quartz-breccia bed from the micaceous-quartzitic sequence.

The white quartzite consists of recrystallised, clear quartz grains (up to 1.5 mm diameter) in a matrix of massive quartzite. The dominant surface is identified as layering because it is not definite that this surface is of a tectonic origin. The quartzite is usually laminated, may be quartz veined and is generally cross-cut by an anastomosing foliation showing grain alignment.

Petrography

The white to buff-coloured quartzite hand specimens are fine grained (BA2) (see Appendix 1 for locations of registered specimens), medium grained (BA5) or medium to coarse grained (BA3) and exhibit a saccharoidal lustre on freshly broken surfaces. Specimen BA2 is a well foliated (less than 1 mm spaced surfaces) rock which is transected by two well-developed jointing sets probably after two foliations. In specimen BA5 the less than 1 mm spaced joint surfaces define the foliation. The laminae vary from 3 mm to 9 mm thick and may be cross laminated(?) as shown by the outcrop from which specimen BA5 was derived.

Table 1
Harrys Bluff — possible tectonic surfaces

Surface	*Description*
S_0	folded into S & Z folds, now intrafolial, produced a cleavage S_1.
S_1	cleavage dipping south.
S_2	mechanical layering, parallel to S_0, thus preserves bedding structures (ripples and cross bedding) but tectonic structures also occur.
S_3	shallowly north or south-dipping cleavage resulting from crenulation of S_1.
S_4	consistent crenulation dipping approximately 50° west, dominant surface in micaceous rocks.
S_5	sporadically developed cleavage trending 060–070°, with a steep dip, also some folds on this trend.

Tectonic surfaces based on the field work of P. R. Williams.

The white to light-grey or greenish-grey micaceous quartzite hand specimens exhibit laminae from 0.25 mm to 2 mm wide (BA1, BA7) and are visibly crenulated. Specimen BA1 shows distinct sigmoidal microlithons, whilst in specimen BA7 the crenulation cleavage is axial planar to the microfolding in the associated outcrop.

Specimen BA6 is a kinked, interlaminated quartzite and greenish-black phyllite in 0.1 mm, 0.2 mm and 0.3 mm thick laminae. Thus dark grey to black mudstone laminae are interlaminated with pale grey 0.5–1.3 mm thick siltstone laminae.

The equigranular monocrystalline quartz grains, which vary in size from 14 m across to 300 m across in quartzite thin section BA2, exhibit undulose extinction and distinct grain boundaries (crossed nicols) which are sutured in the larger grains. In contrast quartzite thin sections BA3 and BA5 consist of two distinct quartz grain sizes; one from 7 to 70 m (50–60% in BA3, 20–30% in BA5) and the other from 175 to 450 m (15–20% in BA3, 50–60% in BA5). In each case the larger quartz grains exhibit sutured margins, elongation (up to 1.5 to 1) but do not contain any granular inclusions marking former grain boundaries. All the thin sections contain some larger quartz grains displaying stripped undulose extinction (usually at an angle to the quartz grain elongation, ?deformation band boundaries) from 21 to 28 m wide in 150 400 m diameter grains (BA2).

HIGH ROUND MOUNTAIN—LONE HILL AREA
EXAMPLES OF CROSS BEDDING/CROSS LAMINATION

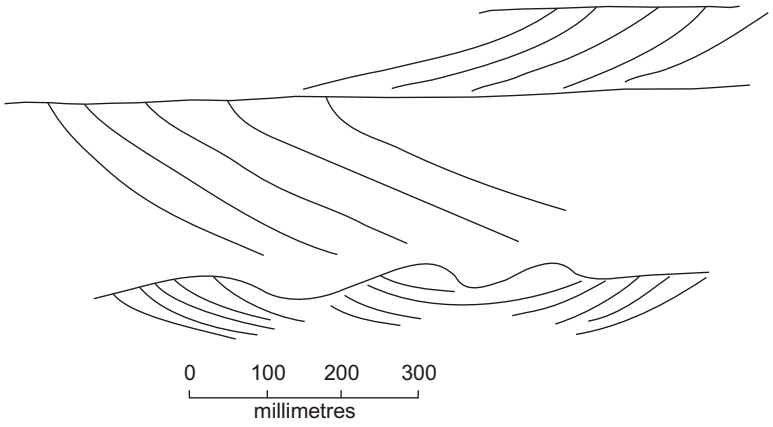

Lone Hill (446700 mE, 5196400 mN)
Possible cross bedding and
ripple-marked quartzite

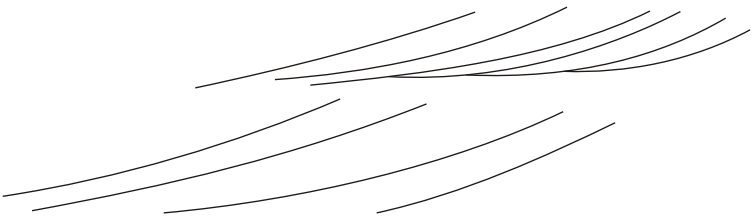

Ngyena Creek ridge
(441600 mE, 5203400 mN)
Two examples of possible
cross lamination within quartzite

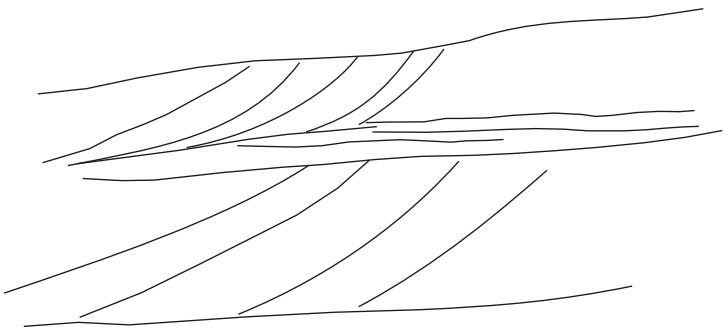

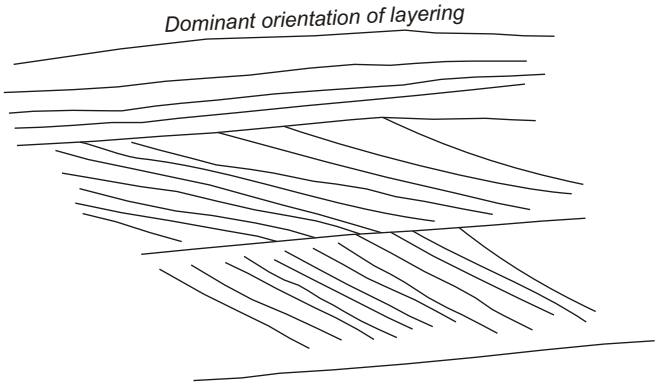

Ngyena Creek ridge
(440000 mE, 5202900 mN)
Planar cross lamination
within quartzite

Figure 3

Table 2

Localities in which quartzite shows possible cross bedding/cross lamination or ripple marks, High Round Mountain–Lone Hill area

1. Localities in which the quartzite shows possible cross bedding/cross lamination. Field station number in brackets.

Ridges off High Round Mountain

444 300 mE, 5 202 600 mN (3)
444100 mE, 5 202 100 mN (5)
442 800 mE, 5 202 500 mN (12)
442500 mE, 5 202 500 mN (13)
444 200 mE, 5 201 300 mN (23)
444200 mE, 5 201 100 mN (25)
443 900 mE, 5 201 100 mN (26)
442900 mE, 5 200 700 mN (29)

Lone Hill

446 700 mE, 5 196 400 mN (77)

Ngyena Creek ridge

441 600 mE, 5 203 400 mN (80)
440 000 mE, 5 202 900 mN (91)
440 500 mE, 5 203 000 mN (89)
442 800 mE, 5 201 600 mN (103)

2. Localities in which the quartzite shows possible ripple marks.

Station	*Co-ordinates*	*Current direction**
3	444 300 mE, 5 202 600 mN	
5	444 100 mE, 5 202 100 mN	from the southeast
77	446 700 mE, 5 196 400 mN	
101	442 100 mE, 5 201 700 mN	from the NE or SW
103 (?)	442 800 mE, 5 201 600 mN	

* The layering surface containing the ripple mark was rotated to the horizontal and the rotations due to tectonic deformations were ignored.

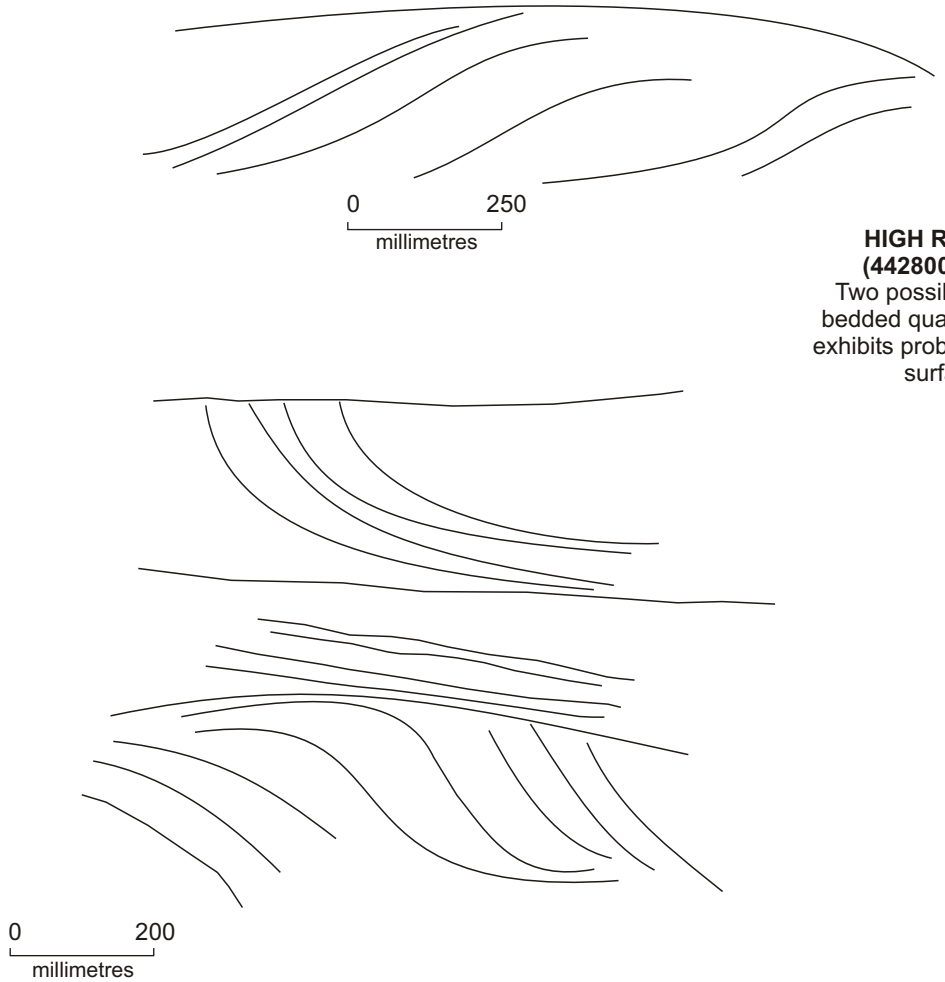

HIGH ROUND MOUNTAIN (442800 mE, 5201600 mN)
Two possible examples of cross-bedded quartzite. This outcrop also exhibits probable ripple marks on the surface of the layer.

Figure 4

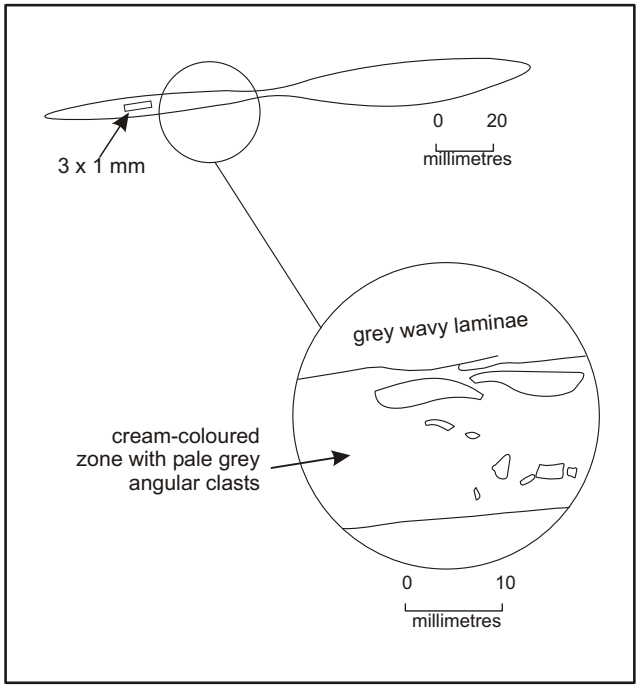

Figure 5

Micaceous quartzite sequence containing quartz-breccia bed within a creek-side cliff section between Harrys Bluff and High Round Mountain (443400/5203900).

The white mica component of the quartzite thin sections varies from 5 to 10% as either individual grains, needles or laths, or in aggregates. The former range from 3 21–35 m (BA5) up to 21 100 m (BA2) and may be randomly orientated (BA3) or aligned parallel to the elongation in the quartz grains (BA5).

The micaceous quartzite thin sections exhibit quartz grains ranging in size from 14 28 m to 49 140 m showing undulose extinction, usually monocrystalline form (BA4, BA7) and some marginal recrystallisation (BA7). Whereas the quartz grains in thin section BA7 are not elongated in the dominant fabric direction those in section BA1 are elongated in this direction. The quartz grains in thin section BA4 are equigranular and monocrystalline. The quartz grain boundaries are usually indistinct, sutured, straight or gently curved. The quartz grains may contain needle-like inclusions (BA4, up to 7 70 m). In plane polarised light the quartz grains form an optically continuous mass whereas in crossed nicols the individual grains are visible. The white mica component of the micaceous quartzite occurs as individual laths or needles or in aggregates of these. In thin section BA1 the white mica forms definite microlithons up to 7 70 m in size, although they are usually about 2 to 4 30 m in size. The differentiated crenulation cleavage in thin section BA7 causes bending of the muscovite(?) lath aggregates. Thin section BA4 contains accessory microcline-twinned plagioclase (up to 720 800 m) with needle-like apatite inclusions.

The phyllite thin section (BA6) contains equigranular quartz grains (up to 21 70 m) exhibiting undulose extinction with straight to gently curved boundaries. The quartz grains may be elongated in the dominant fabric direction which is pervasive.

Structural geology

Layering

As noted before it is probable that the dominant layering observed in the field is of a tectonic origin. On the basis of Williams' mapping in the Harrys Bluff area the layering is probably the second tectonic surface and because it is parallel to the bedding it has preserved on it a number of bedding structures.

Figure 6 is a contoured stereoplot of the poles to layering for the ridges surrounding upper Ngyena Creek. The antiform fold corresponding to the girdle as shown has an axis plunging 17° to 302°. Although some of the foliations measured in the same outcrops are (sub)parallel to the fold axis, many are at a high angle to it.

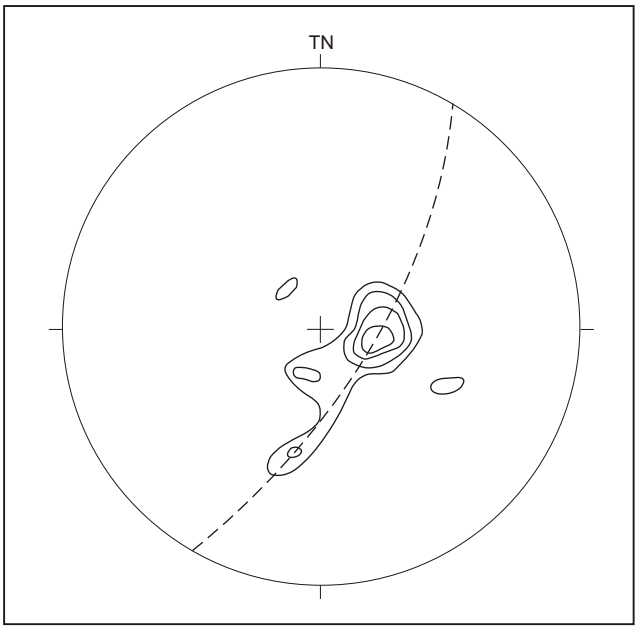

Figure 6

Contoured stereoplot of the poles to layering (31 readings), Ngyena Creek antiform. Contours 6–10–13–16% per 1% area. The fold corresponding to the girdle as shown has an axis plunging 17° to 302°.

Figure 7 shows two (contoured) stereoplots of poles to layering and foliations in the High Round Mountain area. It is apparent from the stereoplot that the dominant layering orientation is a northeast-trending, gently northwest-dipping surface in this area. The stereoplot of the poles to foliation shows a wide scattering from gently dipping to steeply dipping north–south to east–west trending foliations. On the basis of Williams' proposed scheme of possible tectonic surfaces in the Harrys Bluff area (Table 1) a number of foliation fields for the High Round Mountain area are shown encircled in dashed lines on Figure 7.

The contoured stereoplot of the poles to layering in the eastern Ray Range and Lone Hill area (fig. 8) corresponds to a fold with axis plunging 20° to between 004° and 018°. This regional fold axis trend is of a more northerly trend compared with that in the Ngyena Creek area. The largest concentration of poles to layering in the Lone Hill area

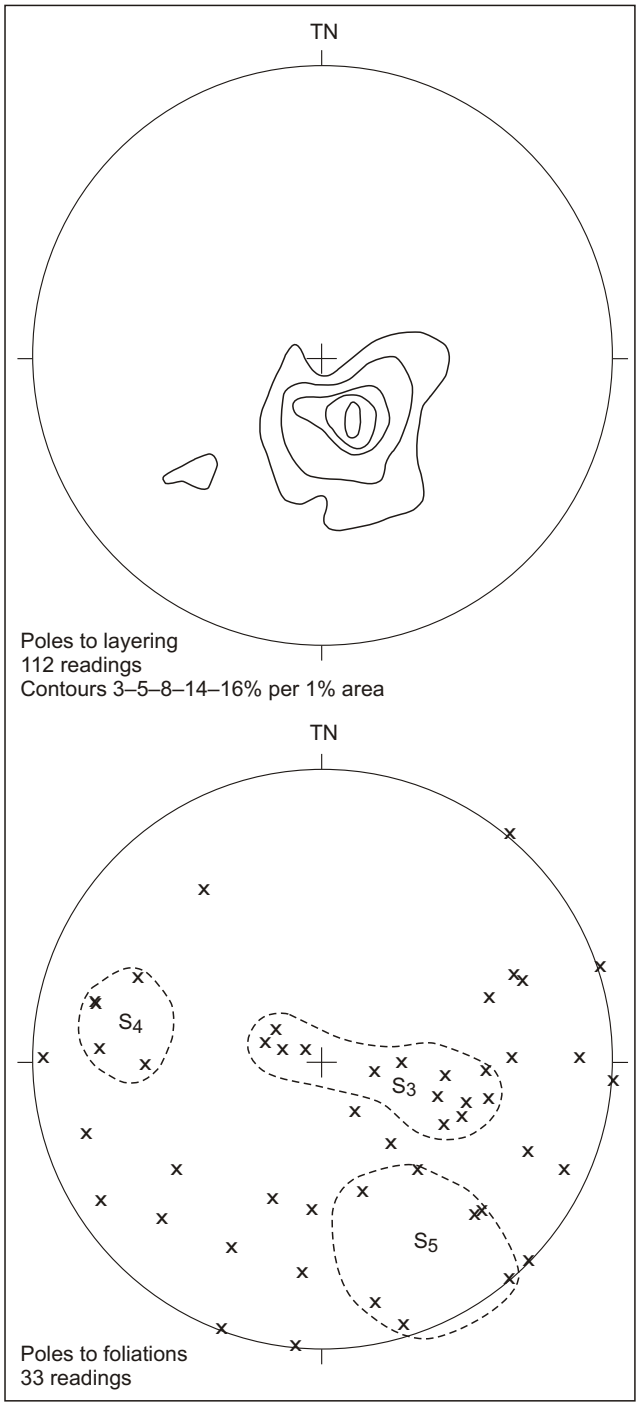

Figure 7

Contoured stereoplot of poles to layering and stereoplot of poles to foliation, High Round Mountain area. Possible tectonic surfaces (S_3, S_4, S_5) may be as shown.

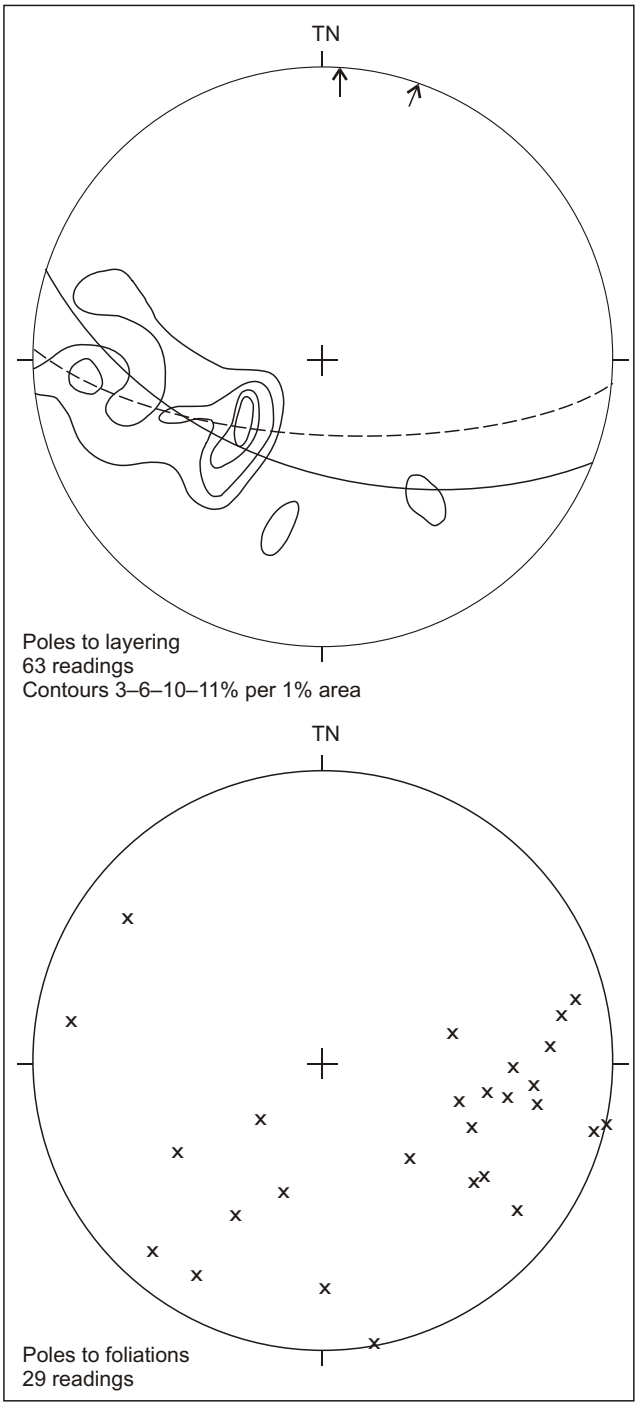

Figure 8

Contoured stereoplot of poles to layering and stereoplot of poles to foliation, eastern Ray Range and Lone Hill areas. The fold corresponding to the full-line girdle has an axis plunging 20° to 018°, whilst the dashed-line girdle corresponds to a fold with axis plunging 20° to 004°. The largest concentration of foliations would be axial planar to the regional fold observed in the contoured stereoplot.

corresponds to a northeast-dipping NW to SE-trending surface. Thus the Lone Hill regional layering trend (NW–SE) differs markedly from the NE–SW trending High Round Mountain regional layering trend.

Foliations

The geological map legend with respect to foliations was prepared on the basis of the observed field relationships between layering and foliations. Three foliations, apart from the dominant layering, were observed; a foliation of unknown relationship to the layering, a foliation cross cutting the layering (either penetrative or crenulate); and a foliation cross cutting the layering and the first foliation.

In the micaceous quartzite hand specimens (BA1, BA7) the secondary foliation is a crenulation cleavage cross cutting the layering. In hand specimen BA1 distinct sigmoidally shaped microlithons are discernible between the 0.5 mm, 1.0 mm and 1.5 mm spaced joint surfaces after foliation surface. In the quartzite hand specimens (BA2, BA5) the

secondary foliation is a number of penetrative joint surfaces after a foliation spaced less than 1 mm to 7 mm apart.

In the quartzite thin sections the fabric is of the disjunctive, anastomosing type according to the Powell (1979) scheme. In the micaceous quartzite thin sections the fabric is either an anastomosing white mica aggregate (BA4) or a differentiated crenulation cleavage (BA1, BA7) (plates 1 and 2). In the former case the white mica aggregates are 45–90–135 m thick and are spaced 450 m apart, whilst in the latter case the quartz-rich microlithons are from 140–210 m wide and the white mica-rich zones are from 14–21 m wide.

In thin section BA1 the degree of differentiated crenulation cleavage development appears to be a function of the proportion of quartz to white mica in the different laminae. The kinked phyllite thin section (BA6) has a crenulation cleavage which may be a differentiated crenulation cleavage in parts of the section (see Plate 3). This cleavage cross cuts the quartz-rich and white mica-rich ribbons defining the layering at a high angle. The white mica-rich zones defining the differentiated cleavage vary in thickness from 100 m to 950 m in thickness and are spaced 500 m apart. They vary along their length by subdivision.

The outcrops from which the hand specimens were collected show three distinct foliations, apart from the layering; N–S trending, NE–SW trending and NW–SE trending. The NW–SE trending foliation is confined to the quartzite specimens whilst the N–S trending foliation is not observed in the collected quartzite specimens. In every case the foliation is either a crenulation cleavage or a differentiated crenulation cleavage. The N–S trending foliation may correspond to the S_4 surface identified by P. R. Williams (Table 1) in the Harrys Bluff area.

Figure 9 shows examples of an outcrop of micaceous quartzite, from near the confluence of the Solly River and Watts River, in which the crenulation cleavage has been

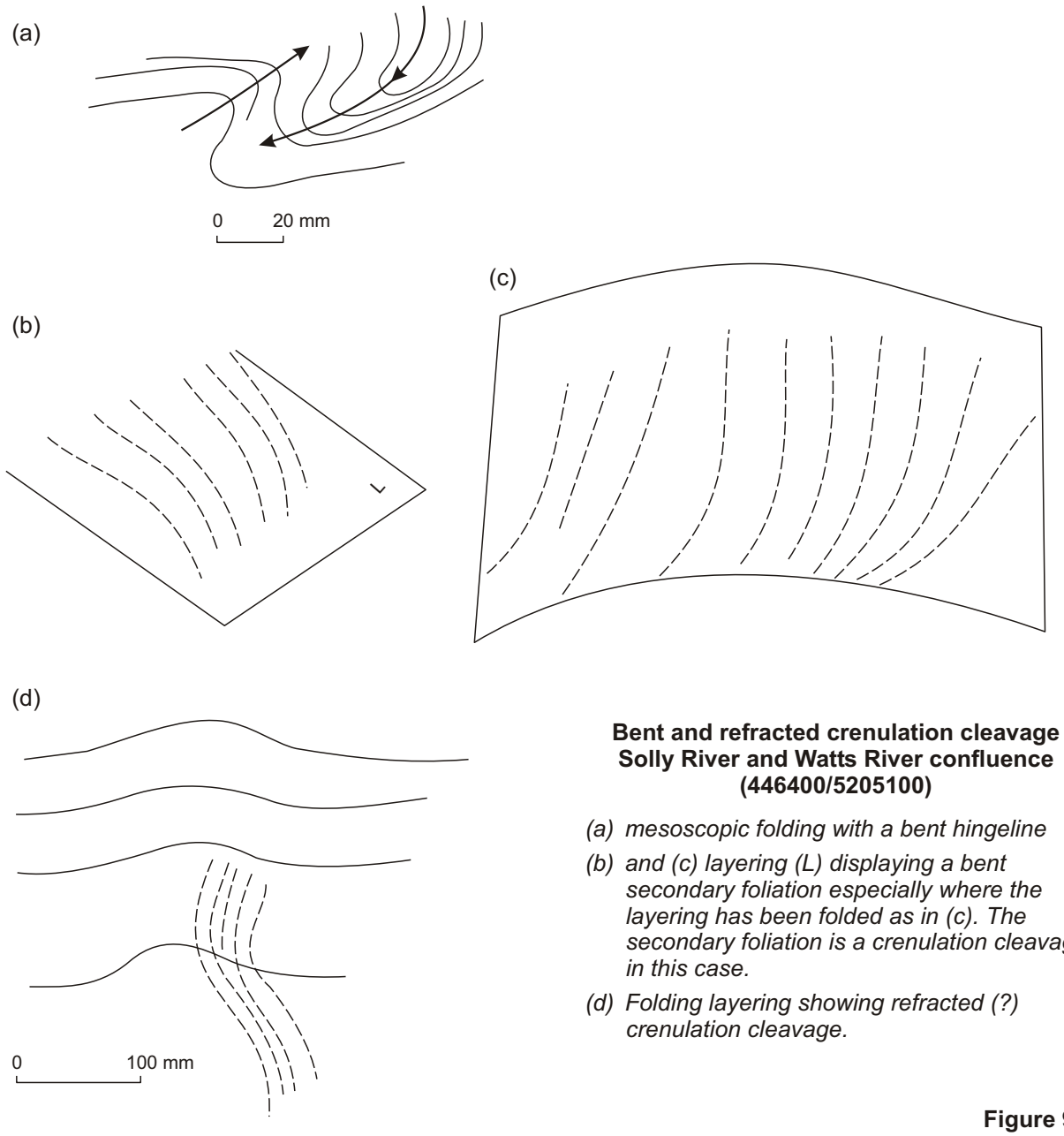

Bent and refracted crenulation cleavage Solly River and Watts River confluence (446400/5205100)

(a) mesoscopic folding with a bent hingeline

(b) and (c) layering (L) displaying a bent secondary foliation especially where the layering has been folded as in (c). The secondary foliation is a crenulation cleavage in this case.

(d) Folding layering showing refracted (?) crenulation cleavage.

Figure 9

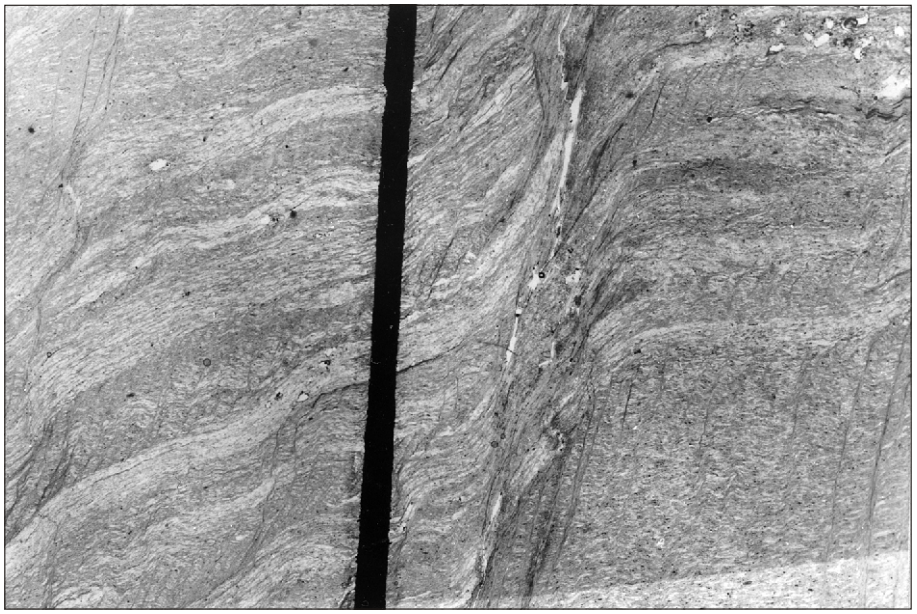

Plate 1
Photomicrograph of micaceous quartzite in ordinary light showing the differentiated crenulation cleavage cross cutting the layering at a high angle. Magnification ~ 5.
Sample BA1, High Round Mountain (441800/5203200).

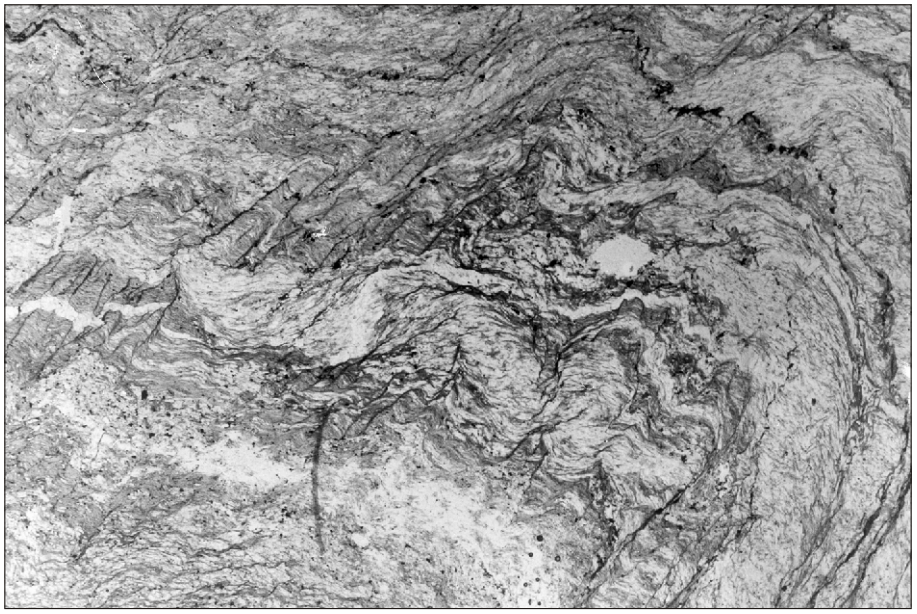

Plate 2
Photomicrograph of micaceous quartzite in ordinary light showing the differentiated crenulation cleavage and kinks which disrupt the layering (dominant foliation).
Sample BA7, lower slopes of Mt Pollux (449000/5203700).

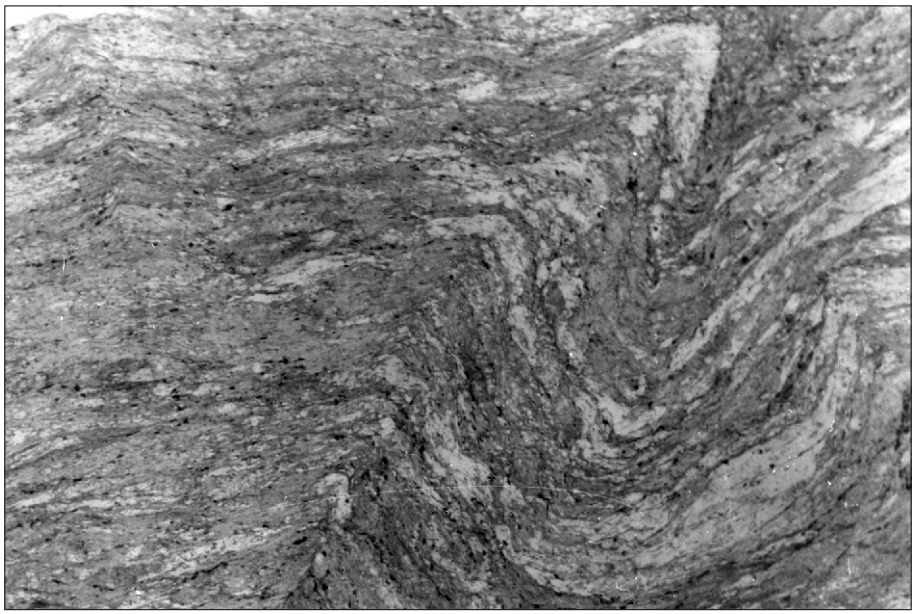

Plate 3
Photomicrograph of phyllite showing the nature of the kinking of the quartz-rich ribbons within the white mica-rich matrix. These ribbons define the layering which is the dominant surface within these rocks.
Sample BA6, eastern end of Ray Range (445500/5195300).

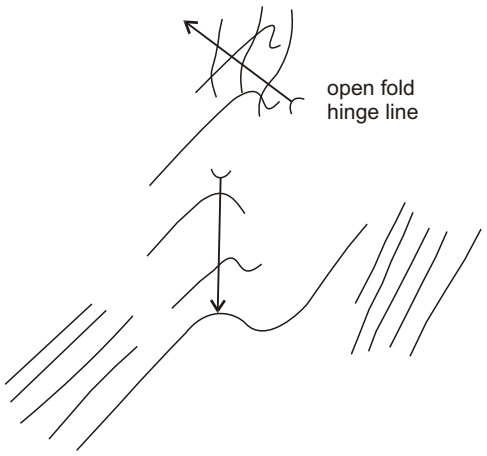

Figure 10

Moderately plunging asymmetric fold cross cut by an open fold at a high angle. The secondary foliation is (sub)parallel to the asymmetric fold hinge line. Lone Hill (446700/5196800).

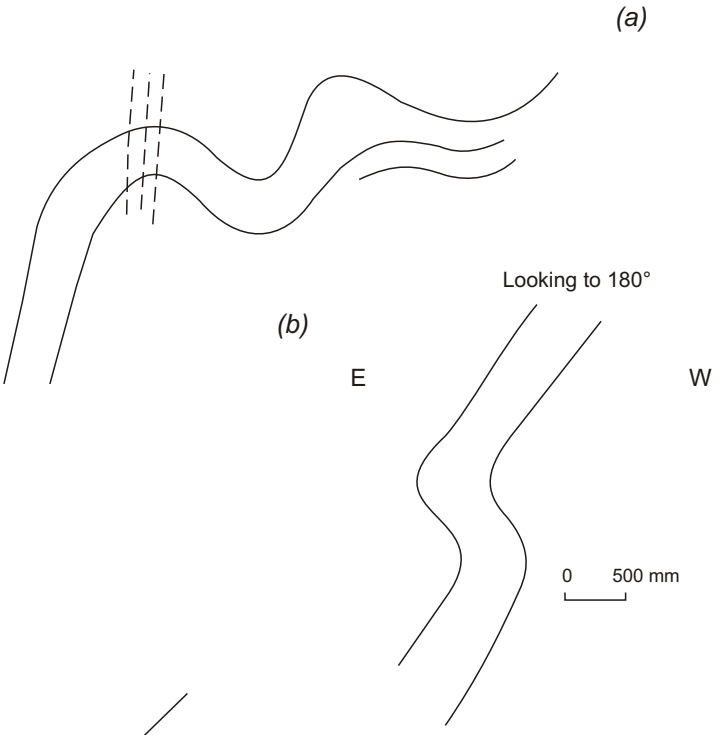

Figure 11

(a) Asymmetric folded 500 mm thick layer with a secondary foliation axial planar to this folding. Ray Range (445100/5194100).

(b) Monocline within a 500 mm thick layer. The fold hinge line plunges very gently to the south. Ray Range (444900/5193600).

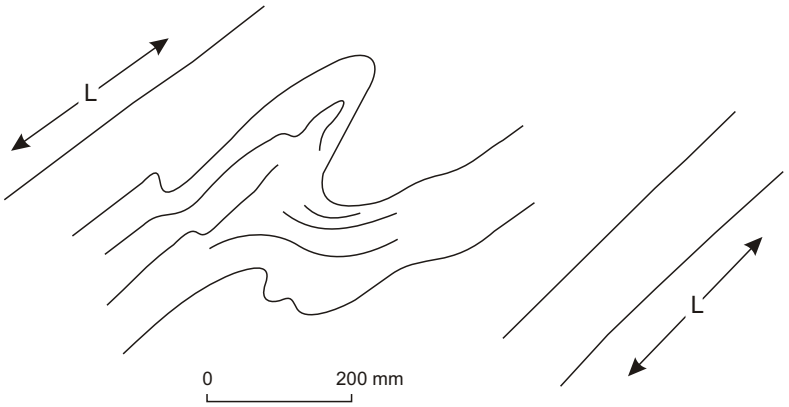

Figure 12

Intrastratal folding of a kinked, layered metaquartzite outcrop which exhibits two secondary foliations, one of which is probably related to kinking. Ray Range (442200/5198400).

bent during folding of the layering. If the layering is the S_2 surface as indicated by the thin section then the associated crenulation cleavage must be S_3 and the folding due to F_4 or F_5. This outcrop also exhibits a probable refracted cleavage in another mesoscopic fold.

Mesoscopic folding

The mesoscopic folds have half-wavelengths ranging from 50 mm to two metres, although most have half-wavelengths less than 100 to 150 millimetres. The most common mesoscopic fold hingelines plunge gently to moderately to the east (west) or southeast (northwest). These folds are usually asymmetric, open (to close), upright folds as shown in the examples from Lone Hill and the eastern end of Ray Range (fig. 10 to 12).

The folds may be dissected by the foliation as seen in figures 13 and 14 from outcrops on the Poimena Hills. The isoclinal fold observed in Figure 14 may be representative of a much larger number of such folds. P. R. Williams (pers. comm.) suggested that some examples of proposed cross bedding my in fact be truncated isoclinal folds.

Kinking

Kinking occurs as both simple and conjugate kinks within the micaceous quartzite exposures in the creek between High Round Mountain and Harrys Bluff (443900/5203600) and in the quartzite exposures near Lone Hill and on Ray Range (442100/5198400). In each case the dominant axial surface trend is either east–west or NW–SE which is the same as the mesoscopic fold hingeline trends. The kinks have axial surface spacings from 50 mm to 200 mm wide and are spaced from 10 mm to 450 mm apart with the overall length not usually exceeding one metre.

In a few case the kinking may be microfolding (Station 67, 445200/5197400 and Station 137, 445400/5195200), whilst in other occurrences the kinking may be associated with a crenulation cleavage (Station 145, 445400/5194600 and Station 180, 442100/5198400).

Summary and conclusions

The metamorphosed Precambrian rocks exposed in the High Round Mountain area consist of either well layered/laminated metaquartzite, micaceous quartzite or phyllite. The layering is probably of a tectonic origin on the basis of the thin sections, although it may have preserved on its surface a number of sedimentary features. The secondary foliations are predominantly crenulate in nature and frequently differentiated crenulates. There are three distinct secondary foliation trends; N–S, NE–SW and NW–SE. The mesoscopic fold hingeline trends and kink axial surface trends are either E–W or NW–SE.

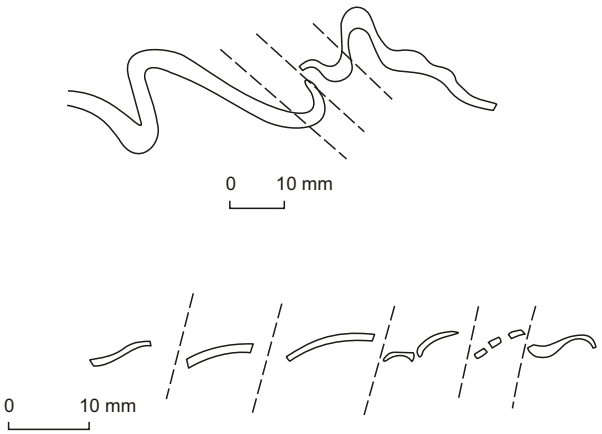

Figure 13

Microfolding of the micaceous quartzite layering with the secondary foliation partly dissecting the layers (upper diagram) and completely dissecting the layers (lower diagram).

Poimena Hills (445700/5203300).

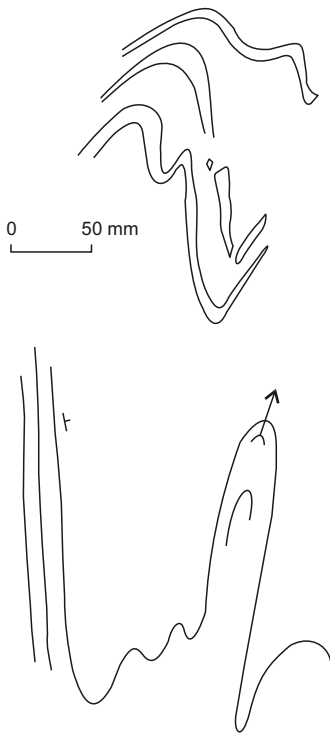

Figure 14

Asymmetric, close folding of the micaceous quartzite layers which are partly dissected (above). The secondary foliation is axial planar to these folds.

Poimena Hills (447600/5202000).

Isoclinally folded micaceous quartzite layers (below). The folds are upright with steeply plunging hinge lines.

Poimena Hills (447800/5201600).

Part B — Louisa Creek area

Introduction

This area includes the Red Point Hills (443000/5181300), Louisa Bay (including Anchorage Cove, 445200/5180400), Quartz Bound Hill (446100/5186800), Spica Hills (448300/5186700) and the Ironbound Range (455400/5182500) where accessible off the South Coast Track. The cliff exposures around Louisa Bay and from Louisa Point (449200/5179300) to New Year Bay (450700/5179400) are precipitous and are difficult to walk. Lack of time prevented mapping of Mt Louisa although this appears to be accessible from upper Louisa Creek and a 'relatively' unvegetated east–west trending ridge. Similarly a lack of time prevented the coastal exposures between Cox Bight and Anchorage Cove from being investigated. These may prove to be as precipitous and difficult to walk as those on the western side of Louisa Bay.

The subdivision of Precambrian units appearing on the Davey 1:250 000 scale geological map (Williams and Corbett, 1977) is based on mapping by Hall *et al.* (1969). Two main sequences are proposed; a metamorphic sequence (pelitic and metaquartzite) and a comparatively unmetamorphosed sequence (conglomerate overlain by orthoquartzite) on the top of the Ironbound Range. The remapping of this region indicates the presence of quartzite units within the pelitic sequence exposed on the Red Point Hills.

Petrography

Metamorphic sequences — pelitic sequence

In hand specimen these laminated pelitic rocks are pale greenish-black (BA8) to greenish-black (BA11, BA15), with occasionally dark grey and black laminated specimens. The 0.1–0.3 mm thick laminae may be clustered in bands (BA12) between four and six millimetres thick, consisting of black muddy laminae and light grey silt to medium-grained sand laminae.

The three hand specimens from Louisa Bay (BA11, 12, 15) exhibit spotting. In thin section BA11 the one millimetre spots are closely spaced and form 35–40% of the specimen, whilst in thin section BA12 the spots range up to 0.5 1.0 mm and are sparsely scattered. In specimen BA19 a 1–2 mm thick iron oxide/hydroxide stained layer contains crystalline pyrite cubes scattered along its length.

In specimen BA15 kinks spaced 5–15 mm apart and of axial surface spacing up to 5 mm are common.

In thin section these pelitic sequence hand specimens consist of interlayered ribbons of aligned bladed white mica-rich layers (as individual blades or in aggregates) and cherty quartz-rich layers (fine-grained quartz grains probably partly to wholly recrystallised) in which the proportion of white mica is high with respect to the proportion of cherty-quartz in the overall specimen. This layering is probably not sedimentary in origin but may be equivalent to the mechanical layering (see Table 1) observed in the Harrys Bluff–High Round Mountain area.

In thin section specimen BA8, which is representative of the group, exhibits layers 70 to 100 m thick. The quartz grains show undulose extinction, usually indistinct intra-quartz grain boundaries and sharp boundaries with the bladed white mica. The quartz grains range up to 140 210 m in size but are usually less than 70 m across. In thin sections BA12 and BA19 elongated lozenge-shaped quartz-rich bodies, up to 1 7 mm in the latter case, occur. In thin section BA12 the large quartz grains contain white mica stringers parallelling the fabric in the white mica. The large quartz grains in section BA19 are usually monocrystalline although some show total recrystallisation. The quartz grains in thin section BA19 may contain granular inclusions and may exhibit white mica bands at their ends. The white mica in sections BA11 and BA15 consists of feathery aggregates of chlorite after muscovite(?). The spots consist of a 'milky looking', generally isotropic mineral (PPL) in thin section BA11 and a mesh containing chlorite, semi-opaque minerals and a high relief isotropic mineral (?garnet) in section BA15.

Quartzites

The generally white coloured (BA9, 13, 24 and 25), sometimes greenish-grey (BA17, BA22) or iron oxide/hydroxide-stained commonly laminated quartzites frequently exhibit a resinous lustre on laminae surfaces due to white mica accumulations. The quartzite laminae range from less than 0.2 mm thick (BA13, BA17) up to 2 mm (BA25) whilst the white mica-rich laminae range up to 0.1 mm thick. Variously developed crenulation cleavage surfaces spaced 1.5 to 2 mm apart cross-cut the dominant lamination in hand specimens BA13, BA16 and BA25. Hand specimens BA13, BA16 and BA22 display saccharoidal quartz grains on freshly broken faces. Hand specimen BA22 has cavities ranging from 1.5 mm to 6 mm in diameter, some of which contain oxidised material.

In thin section these specimens differ from the pelitic sequence in the low proportion of white mica-rich ribbons compared with cherty quartz-rich ribbons. The thin sections of samples BA16, BA24 and BA25 indicate the rocks to be completely recrystallised quartzite. In thin section BA9 the white mica ribbons consist of aligned muscovite laths and occasional opaque seams spaced 70 to 350 m apart.

The quartz grains invariably show undulose extinction, commonly straight distinct grain boundaries, and have 120° angles at quartz grain triple junctions. These features are indicative of the usually large degree of recrystallisation these rocks have undergone during deformation. In thin sections BA17, BA24 and BA25 the quartz grains are elongated up to 2:1. In section BA25 there are two discernible grain sizes; one group of quartz grains up to 35 m across (cherty quartz) interspersed between the other group of quartz grains which are monocrystalline and range up to 150 m across. This pattern indicates the onset of recrystallisation of the quartz grains. The totally recrystallised quartzite thin sections BA17 and BA24 have quartz grains generally less than 70 m across in size,

although some quartz grains range up to 140 m across. Section BA24 is unusual in that the quartz grains appear to be elongated at right angles to the layering.

The white mica component of these sections ranges from <1% (BA16) up to 5–7% (BA9, BA25) and is probably muscovite as aligned individual blades or in aggregates. The bladed white mica aggregates range from 7 70 m (BA17) up to 21 140 m (BA19) to 210 350 m (BA17).

In thin section BA16 rare blocky, slightly elongated twinned feldspar grains from 35–70 m 140 m to 140 m across occur ensheathed in a less than 3 m white mica-rich zone. The twinning is of the albite-carlsbad type.

Comparatively unmetamorphosed sequence

One quartzite hand specimen (BA10, 455800/5182800) was collected from this sequence near the top of the Ironbound Range. As the specimen has been lost no petrographic description can be prepared.

Stratigraphy

As noted in the introduction the metamorphic sequence has been subdivided into a pelitic sequence and a metaquartzite sequence on the basis of the regional mapping of Hall *et al.* (1969). The metaquartzite sequence and the quartzite horizons within the pelitic sequence are invariably layered or laminated (layers from 10 to 60 mm thick) and frequently show a marked change in thickness laterally from about 5 mm thick up to 60 mm thick. This variation may be due to boudinage. The quartzite is usually a white, medium-grained recrystallised rock with a saccharoidal appearance on the freshly broken faces. The typical exposure consists of lenses of recrystallised quartzite in a friable medium sand grain matrix. Table 3 lists the localities in the metamorphic sequence where the quartzite shows possible cross bedding or cross lamination. An example of cross lamination from the metaquartzite on the South Coast Track is shown in Figure 15.

The Louisa Bay exposure on the cliffs and foreshore platform between Louisa Creek and Louisa River contains the probable load and flame structure shown in Figure 16. Plate 4 shows the typical layering with kinking exhibited by the pelitic sequence in Louisa Bay, whilst Plate 5 shows a unique 170 mm to 50 mm wide breccia lense also exposed in this part of Louisa Bay.

The comparatively unmetamorphosed sequence exposed near the top of the Ironbound Range, usually above the 700 m contour, consists of a quartz-conglomerate sequence overlain by a quartzite sequence. The conglomerate contains angular to platy or tabular cobbles to small boulders of cleaved/uncleaved quartzite randomly arranged in a medium sand-sized quartzite matrix. The conglomerate sequence in one exposure consists of a 500 mm thick bed graded from cobble to grit interbedded with a 0.5 to 1.0 m thick bed of angular cobble-sized quartzite clasts without visible sorting or grading in a quartzite matrix. The conglomerate may have a pink tinge resembling that exhibited by the Ordovician quartz-conglomerate exposed elsewhere in Tasmania.

Table 3
Louisa Creek area

Metamorphic sequence: Localities in which the quartzite shows possible cross bedding/cross lamination. Field station number in brackets.

Ironbound Range	453 800 mE; 5 182 700 mN (214)	upside down
South Coast Track	446 200 mE; 5 185 700 mN (291)	upside down
	445 300 mE; 5 185 900 mN (294)	upside down
	444 700 mE; 5 185 800 mN (296)	upside down
Red Point Hills	444 200 mE; 5 184 800 mN (305)	
	444 900 mE; 5 184 000 mN (314)	
	445 200 mE; 5 183 800 mN (317)	right way up
Spica Hills–Quartz Bound Hill		
	448 900 mE; 5 184 500 mN (245)	right way up
	448 700 mE; 5 186 000 mN (252)	right way up
	447 100 mE; 5 187 100 mN (269)	right way up
	447 100 mE; 5 186 200 mN (275)	
Louisa Point	449 100 mE; 5 179 700 mN (284)	

Comparatively unmetamorphosd sequence: Localities in the Ironbound Range in which the orthoquartzite shows current ripples or grading.

Station	*AMG co-ordinates*	*Description*
221	456 700 mE; 5 183 100 mN	grading, right way up
223	457 000 mE; 5 183 200 mN	current ripples, current from the NW or SE*

* The bedding surface (?) containing the ripple mark was rotated to the horizontal and the rotation due to tectonic deformations was ignored.

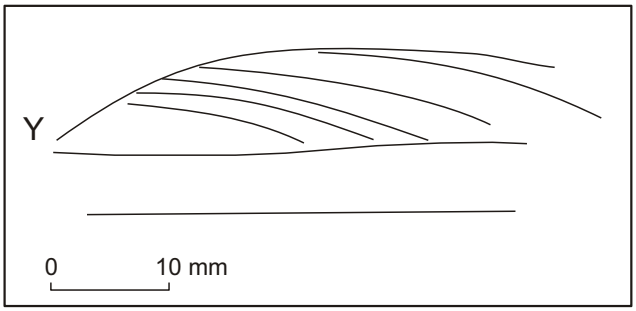

Figure 15
Cross-laminated quartzite within the pelite sequence indicating that the sequence is upside down. South Coast Track near Louisa Creek (446300/5185500).

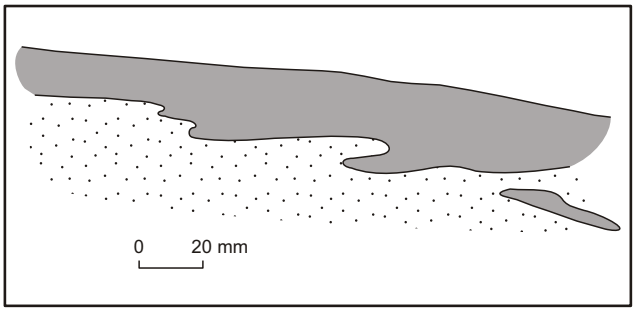

Figure 16
Metamorphosed Precambrian pelite with a dark grey coloured silt bed above and a lighter grey-coloured silt bed below, with a load and flame structure between. Louisa Bay (447500/5181400)

Plate 4
Precambrian pelitic sequence at Louisa Bay (447300/5181400) showing typical layering with kinking (left of geology pick) and folding within distinct belts. Note the lack of folding in adjacent areas.

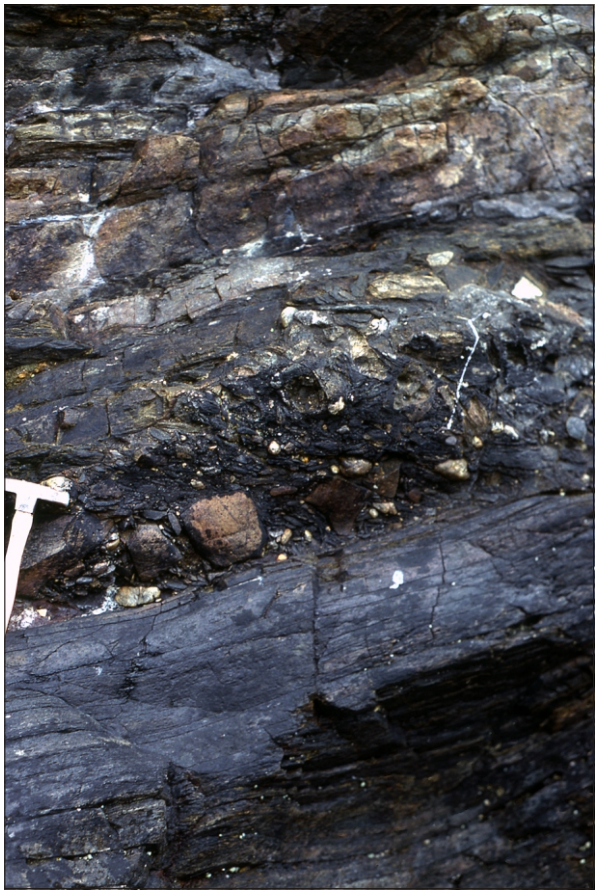

Plate 5
Precambrian metamorphic rocks–pelitic sequence at Louisa Bay (447600/5181500) with a breccia lense from 170 mm to 500 mm wide and over five metres long.

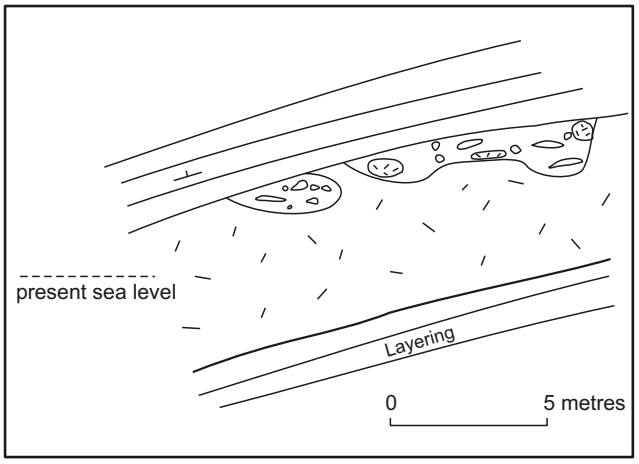

Figure 17
Quaternary(?) partly consolidated deposit two metres above present sea level on the foreshore platform at the contact between a dolerite sill and sediments, Louisa Bay near Anchorage Cove (446100/5181100).

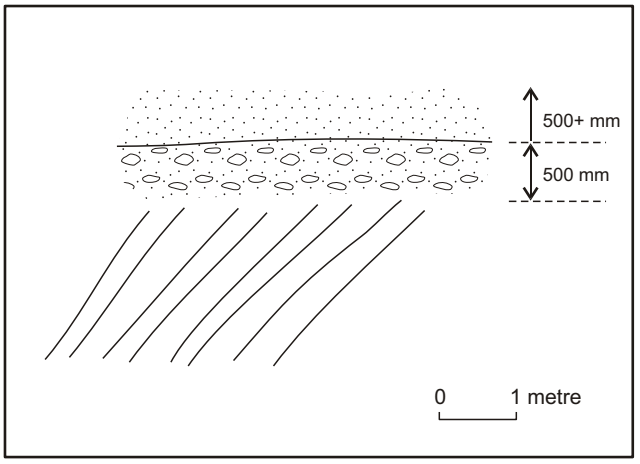

Figure 18
Five to seven metre thick pelitic sequence overlain by an up to 500 mm thick quartz-pebble gravel which is in turn overlain by 500 mm+ of sand. Louisa Bay near Louisa Creek (447200/5181500).

The conglomerate exposed on the north–south trending ridge at the western end of the Ironbound Range (454500/5181900) appears to be faulted out against the metaquartzite of the remainder of the ridge.

The quartzite overlying the conglomerate consists of pink tinged or white, well-bedded quartzite. The beds range from 20 mm to 400 mm thick. The medium-grained quartzite beds may be interbedded with thin bands of a more fine-grained siltstone in some exposures.

There are three exposures of isolated boulders of quartz-pebble to cobble conglomerate within button grass plains which are probably transported equivalents of the comparatively unmetamorphosed quartz conglomerate exposed near the top of Mt Louisa and the Ironbound Range. The cluster of one to two metre diameter boulders adjacent to Louisa Creek (446800/5186100) and adjacent to the Spica Hills (447700/5184900) consist of angular, platy to well rounded, pebbles to cobbles of quartzite in a medium sand-sized quartzite matrix. The up to three metre diameter cluster of boulders adjacent to Louisa River (452000/5184800) contains layer clasts compared with the previously described boulders. One large boulder contains angular platy to tabular cobbles, small boulders and boulders of cleaved, sometimes folded quartzite in a medium sand-sized quartzite matrix.

There are four exposures in the Louisa Bay area in which the pelitic sequence displays spotting: from west to east the Anchorage Cove foreshore (445800/5180800); between Louisa Creek and Louisa River (447200/5181500 and 447900/5181400); and Louisa Island (448000/5179600). The spotting varies in intensity and the spots are usually confined to one layer within an unspotted group. The spotting is not related to the dolerite dykes which are exposed elsewhere in this bay. The invariably pink to light brown coloured spots (BA11) are from 0.5 mm to 2 mm in diameter and usually appear undeformed. The spotting in specimen BA19 appears to be elongated parallel to the foliation lineation.

Dolerite sills associated with the pelite sequence

There are two dolerite sills near Anchorage Cove; one five metres wide (446100/5181100, BA20) and the other ten metres wide (446300/5181200). In the former case the extremely weathered dolerite exhibits the same secondary foliation as that in the enclosing sediments and there is no visible grain size variation across the sill. There is evidence of a former shoreline(?) with unconsolidated deposits of pebbles to boulder-sized clasts of angular, planar (imbricated) pelite and tabular dolerite and pebbles of well rounded vein quartz in a friable medium quartz-grain (well rounded grains) matrix near the upper dolerite–sediment contact which is about two metres above the present sea level (see Figure 17).

The extremely weathered, greenish-black, medium-grained hand specimen BA20 exhibits an excellent cleavage fabric. In thin section there are minor relict amphibole(?) crystals up to 70 140 m in size and minor altered, simply twinned laths after plagioclase within an aligned, feathery chlorite(?) matrix. The same metasomatic alteration exhibited by the Eocambrian Cooee Dolerite on the northwest coast of Tasmania is evident in this thin section.

Quaternary(?) quartz gravel deposit

The exposure shown in Figure 18 occurs on the cliff outcrop near the Louisa Creek mouth in Louisa Bay. The partly consolidated, well-rounded quartz pebble to small cobble gravel is overlain by a sand deposit over 500 mm thick. This sand forms the base of the sometimes very thick dunes which occur in parts of Louisa Bay.

Structural geology

Layering

The thin sections show that it is probable that the layering is tectonic in origin, in a similar fashion to the observed layering in the High Round Mountain area described in Part A of this report.

A number of major folds with half-wavelengths between 0.5 and 1.25 km have been delineated in the Red Point Hills area, both north and south of the South Coast Track (444000/5185600). These generally north–south trending folds are truncated against east–west trending faults. Figure 19 is a collection of contoured stereoplots of the poles to layering in the Red Point Hills area. Thus north of the South Coast Track there is a synform with axis plunging 25° to 170° which is truncated by an east–west fault. In the area north of Ravine Creek (445000/5183300) but south of the South Coast Track an antiform and synform complex was delineated. The more westerly situated antiform has an axis plunging 6° to 017° whilst the more easterly situated synform has an axis plunging 10° to 191°. This couplet is truncated to the north and south by east–west trending (transcurrent?) faults. At the southern end of Red Point Hills a synform with axis plunging 10° to 011° has been identified. This may represent the displaced continuation of the synform delineated above. If this is the case it would imply that the fault is a dextral transcurrent fault.

Figure 20 shows the (contoured) stereoplots of the poles to foliations for the three sub areas identified from the Red Point Hills area. The dominant secondary foliation from these plots is (sub)parallel to the axis of the folds. The few mesoscopic fold hingelines are aligned predominantly east–west, whilst the kink axial surface may be aligned either approximately north–south or east–west.

Figure 21 is a contoured stereoplot of the poles to layering for Quartz Bound Hill and the western side of Spica Hills. Although the girdle is not well defined, the possible antiform may have an axis plunging 20° to 016° or 196°.

The upper stereoplot in Figure 22 shows the poles to foliations and axial surface of kinks in the same area as the data used to construct Figure 21. There appears to be two secondary foliation trends (primary foliation is the layering); one (sub)parallel to the possible fold axis (north–south) and the other trending NW–SE.

The data from the pelitic sequence between Anchorage Cove and New Year Bay in the Louisa Bay area is shown in the lower stereoplot of Figure 22. The dominant layering orientation is a layer trending NE–SW and dipping moderately to the northwest. The dominant secondary foliation trends about NW–SE, whilst the dominant kink axial surface trend is about E–W to NW–SE.

Overall it appears that if the layering represents the second tectonic surface then the third generation folding and foliation (kinking) is aligned north–south in the Louisa Creek area. A later foliation trends NW–SE and mesoscopic folding and kinking are associated with another deformation (later than D_3) trending east–west.

In Figure 23 the upper stereoplot shows data for the metamorphosed Precambrian quartzite on the Ironbound Range, whilst the lower stereoplot shows data for the overlying comparatively unmetamorphosed sequence on top of the Ironbound Range. The dominant layering trend from the sparse data in the former case is a surface trending about north–south and dipping moderately to the east, whilst the dominant secondary foliation trend is similarly aligned.

The comparatively unmetamorphosed sequence bedding is gently east dipping and north–south striking, whilst the few cleavages measured are more steeply east dipping and north–south striking in orientation.

Foliation petrography

Plates 6 and 7 are examples of the nature of the different secondary foliations present in the metaquartzite exposures from Spica Hills and the Ironbound Range respectively. The metaquartzite from Spica Hills shows a well developed mechanical layering cross cut by a well developed differentiated crenulation cleavage, whereas the metaquartzite from the Ironbound Range exhibits anastomosing opaque stringers as the dominant secondary foliation (taking the layering as the primary foliation). Many of the metaquartzite sections (BA16, BA17) have a minor white mica component so that the elongation of the quartz grains and occasional aligned bladed muscovite are the only indications of a secondary fabric. In sections BA17 and BA25 a crenulation cleavage spaced 900 m to 1260 m apart cross cuts the mechanical layering at a moderate angle.

The quartzites are invariably recrystallised with or without elongated quartz grains and similarly aligned individual needles or aggregates of white mica (usually muscovite). The primary foliation resembles that exhibited by specimens with a higher white mica component in that there is a tendency towards the formation of ribbons which are either quartz rich or white mica rich. The nature of the primary foliation in this region resembles that observed in thin sections of metaquartzite from the High Round Mountain area.

Plates 8 and 9 are examples of the nature of the secondary foliation and primary foliation within pelitic sequence thin sections from Louisa River and Louisa Bay respectively. In the former case the widely-spaced crenulation cleavage cross cuts the primary foliation (layering) at a high angle whilst in the latter case the extremely penetrative primary foliation results in the development of tapering quartz-rich lozenges within the white mica-rich matrix.

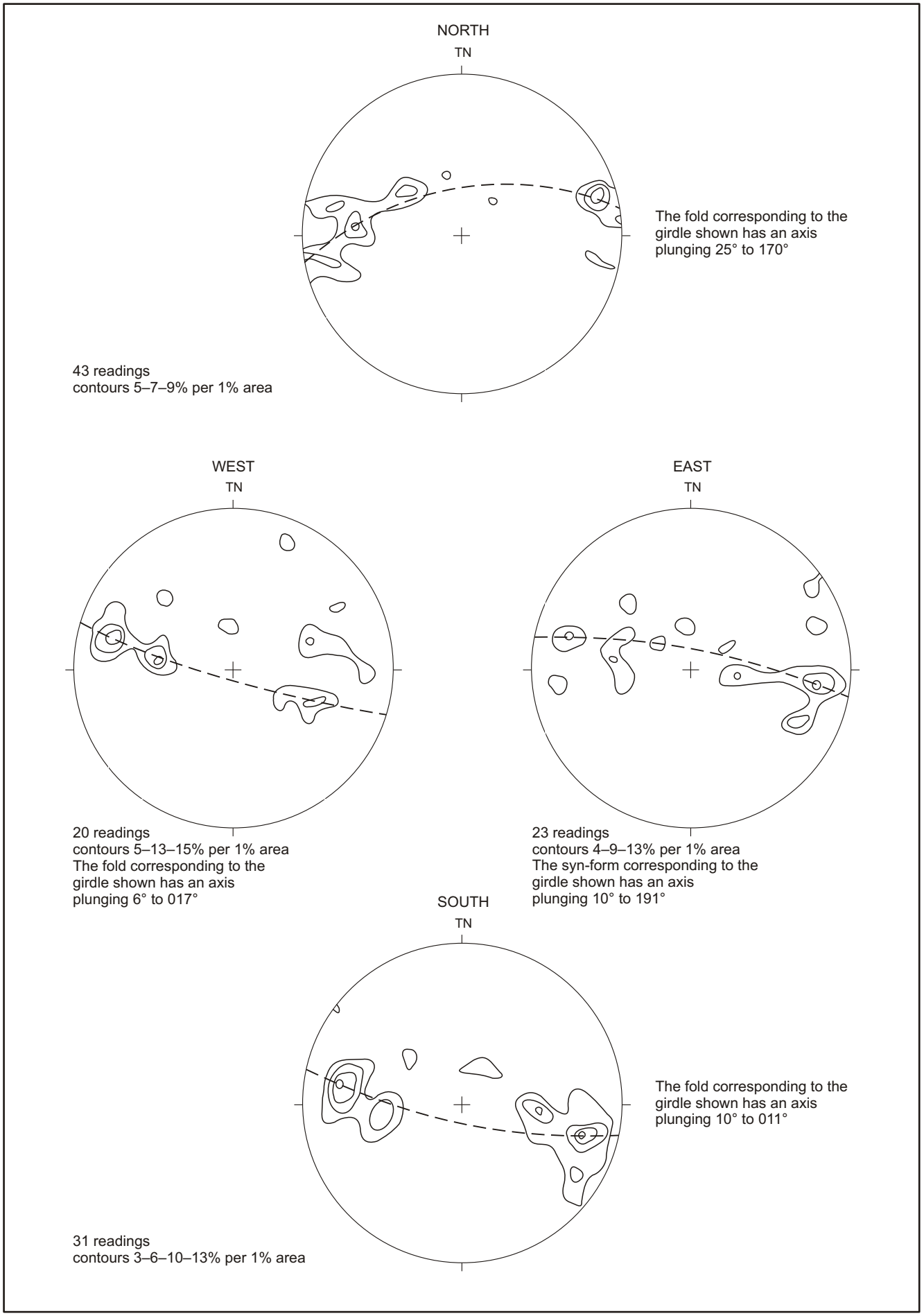

Figure 19

Contoured stereoplots of poles to layering, Red Point Hills

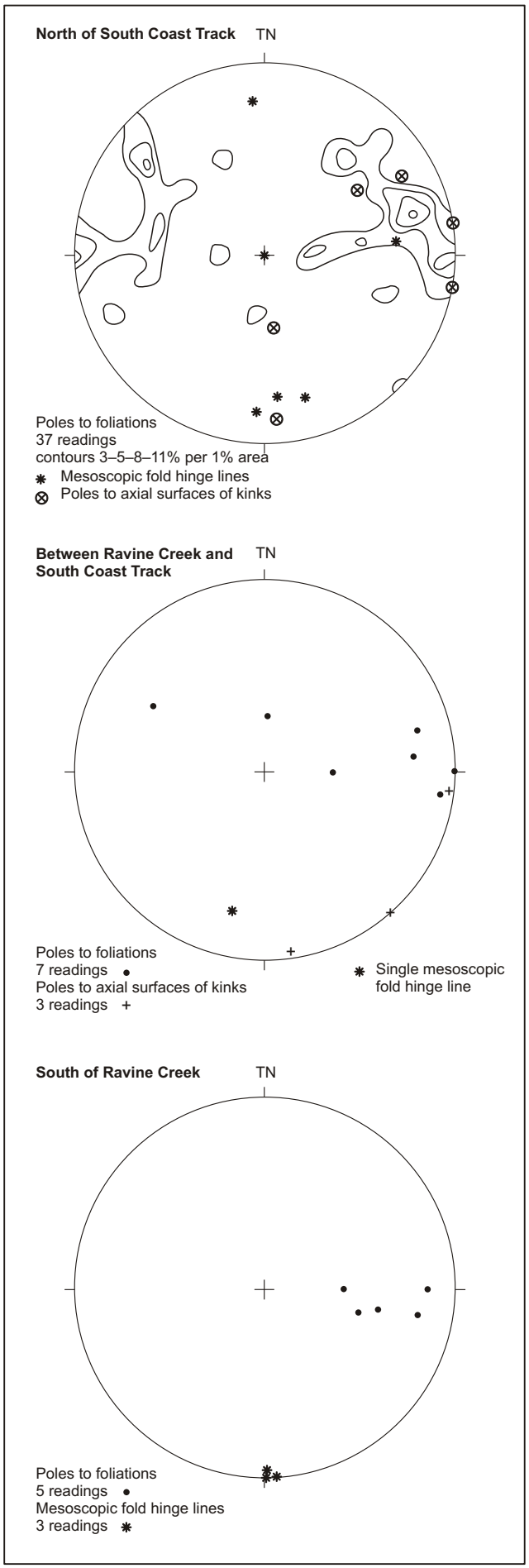

Figure 20
Stereoplots, Red Point Hills

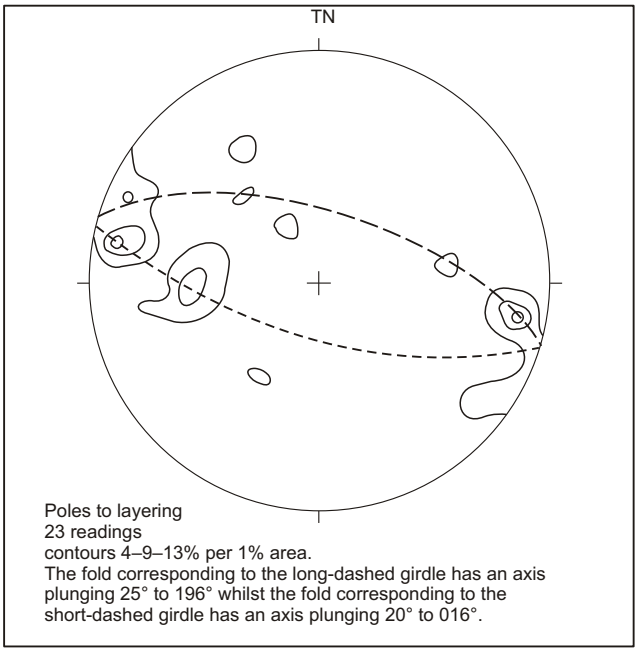

Figure 21
Contoured stereoplot of poles to layering, Quartz Bound Hill and western side of Spica Hills

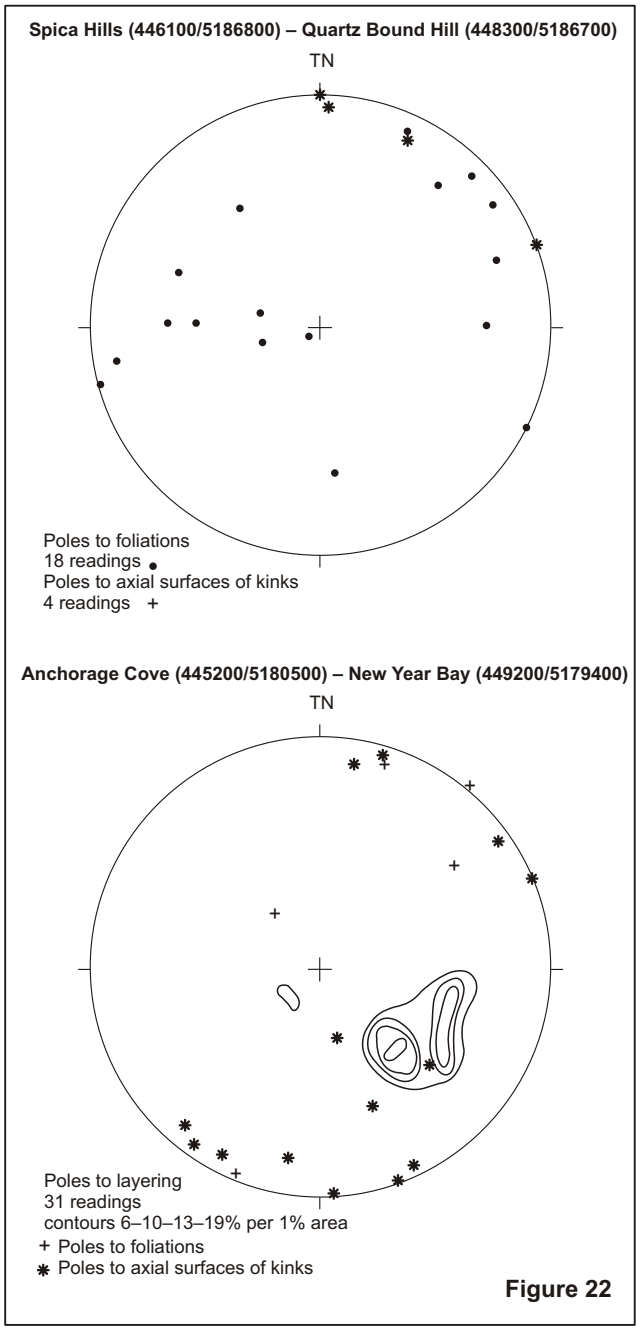

Figure 22

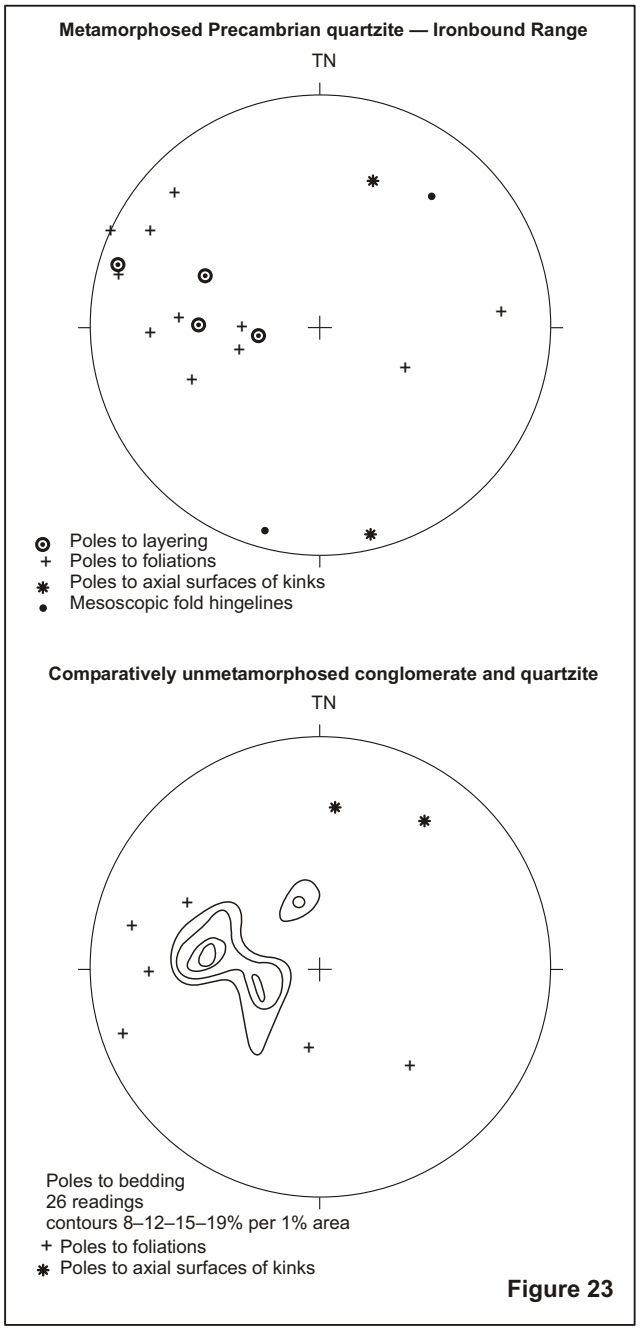

Figure 23

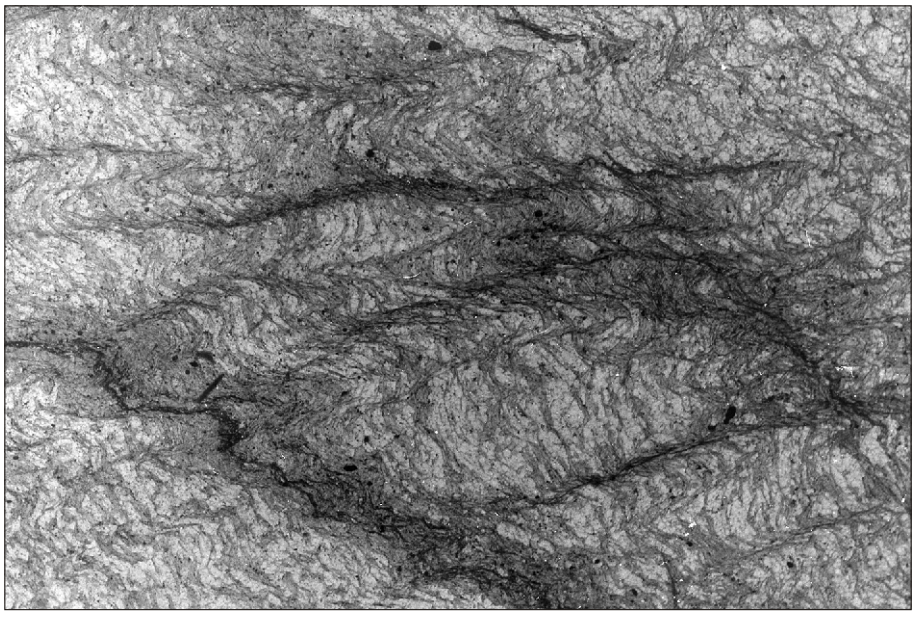

Plate 6

Photomicrograph of metaquartzite showing the development of a differentiated crenulation cleavage at a high angle to the layering. The spacing between the semi-opaque to opaque differentiated zones varies between 1.5 mm and 2 mm.
Sample BA13, Spica Hills (448800/5185300).

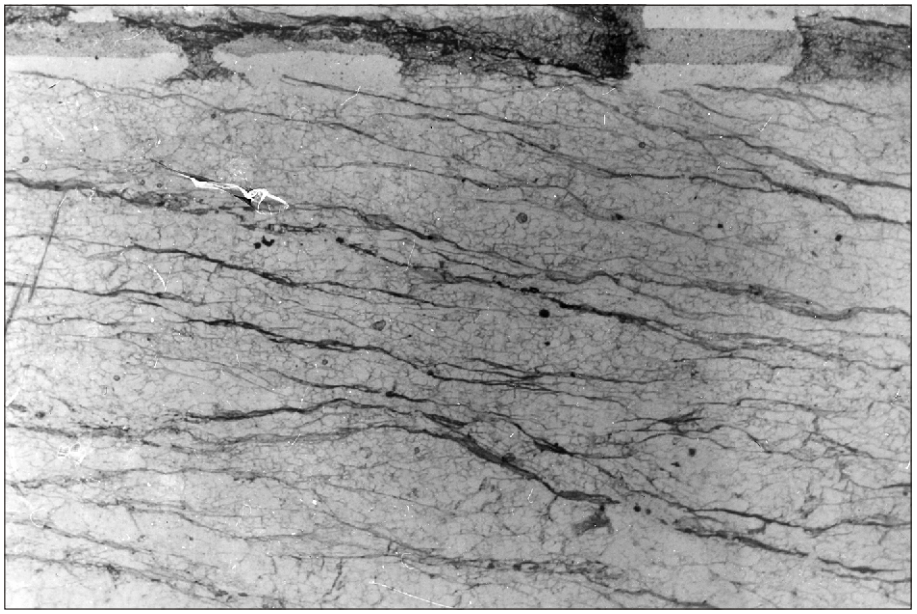

Plate 7

Photomicrograph of a metaquartzite showing the disjunctive, anastomosing opaque stringers defining the cleavage fabric. Sample BA22, Ironbound Range (454700/5180900).

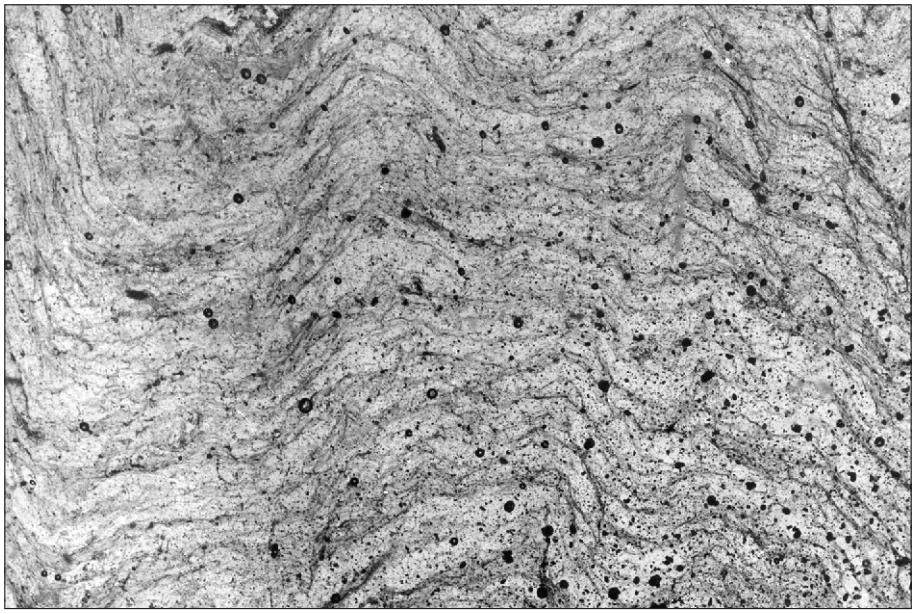

Plate 8

Photomicrograph in ordinary light of a laminated pelite showing a well-developed crenulation cleavage spaced 1–2 mm apart. The layering consists of quartz-rich ribbons between white mica-rich ribbons from 70 to 100 m thick.
Sample BA8, Louisa River (452400/5184500)

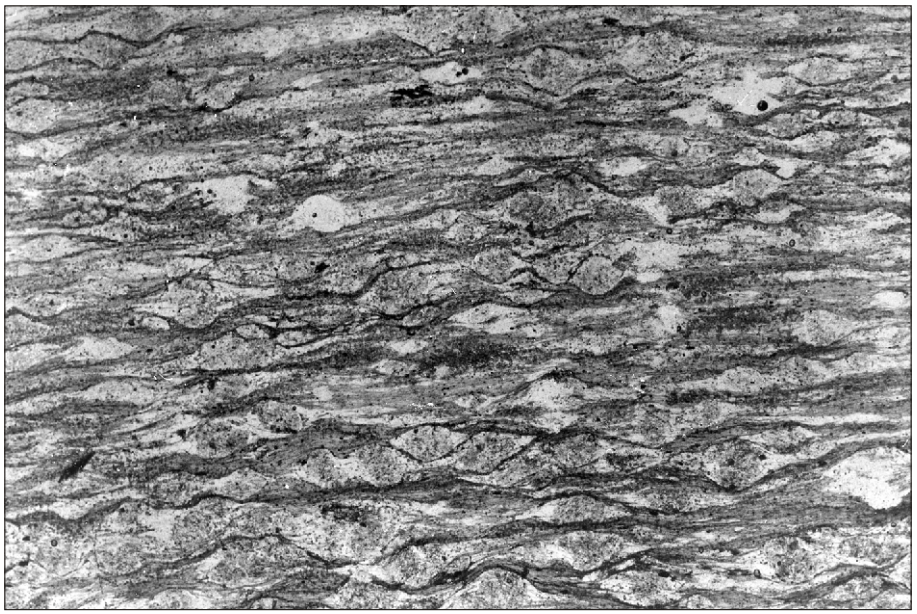

Plate 9

Photomicrograph of quartz-rich tapering lozenges within a predominantly white mica-rich matrix. Although not visible in this plate there is a weakly developed cross-cutting spaced cleavage at a high angle to the pervasive white mica fabric shown.
Sample BA12, Louisa Bay (447300/5181600)

Mesoscopic folding

As has been noted previously in the Red Point Hills area the major fold axes and dominant secondary foliation trend approximately north–south, whereas the mesoscopic fold hingelines trend east–west. It thus appears that the mesoscopic folding is related to a post D_3 deformation. These mesoscopic folds are usually gently to moderately plunging, upright asymmetric folds but may occasionally be recumbent or upright, isoclinal folds. Figures 24 and 26 are examples of the style of folding observed in the Red Point Hills area.

The small mesoscopic folding shown in Plate 4 is typical of that exhibited by the pelitic sequence on the foreshore cliffs and platform at Louisa Bay. The flow-like folding observed near the geology pick is truncated against a normal fault. Figures 30 and 31 are examples of the asymmetric folding and 'ptygmatic like' folding observed in the pelitic sequence in the Louisa Bay area.

Only a few mesoscopic folds were observed in the metaquartzite sequence exposed on the Ironbound Range. Figures 25, 28 and 29 are examples of the asymmetric, upright, gently plunging mesoscopic folds observed from the metaquartzite sequence on the Ironbound Range.

Kinking

Kinking is observed in both the metamorphosed Precambrian sequences; the metaquartzite sequence on Spica Hills and the lower Ironbound Range and the pelitic sequence exposed on the Red Point Hills and around Louisa Bay. The kinks are usually simple, although conjugate kinks were observed in a pelitic layer from the banks of Louisa River (452300/5184400) and Louisa Bay (see Plate 12). The majority of kinks have an axial surface spacing of from 5 mm to 150 mm, although most are in the range from 20 mm to 50 mm. On Louisa Island (448400/5179500) the pelitic sequence exhibits abundant kink bands as shown in Plate 10.

The lower stereoplot of Figure 22 shows that the dominant kink axial surface trend in the Louisa Bay area, where the layering strikes NE–SW and dips moderately to the NW, is east–west to NW–SE. The dominant kink axial surface trend in the Red Point Hills area north of the South Coast Track, where the layering strikes about north–south, is NNW–SSE or east–west. A comparison of these layering–kink axial surface relationships appears to indicate no apparent simple relationship.

The wisps of quartz shown in Figure 27 are truncated by the kinks.

Faulting

A NW–SE trending fault about six kilometres long (443800/5187500 to 448900/5184600) is clearly definable in the Red Point Hills to Spica Hills area on the basis of the lithological change and variation in relief. This fault truncates the metaquartzite sequence to the north against the pelitic sequence with metaquartzite layers to the south.

The Red Point Hills are dissected by three 2 to 3 km long about east–west trending faults, one or two of which may be dextral transcurrent in character. The faults truncate major folding in this area and are reflected in the distinctive gullies down which minor creeks have formed.

Plates 11 and 12 are from the foreshore cliff exposure on Louisa Bay (447300/5181400) where a possible thrust fault has disrupted the layering.

The boundary between the metaquartzite sequence and comparatively unmetamorphosed conglomerate and quartzite on the Ironbound Range appears to be erosional; in most areas, although on the north–south trending ridge at the western margin of the range it may be a fault.

Plate 10
Kink bands from the pelitic sequence on Louisa Island (448400/5179500). These spaced anastomosing kink bands were abundant over a 500 m long foreshore section.

Plate 11

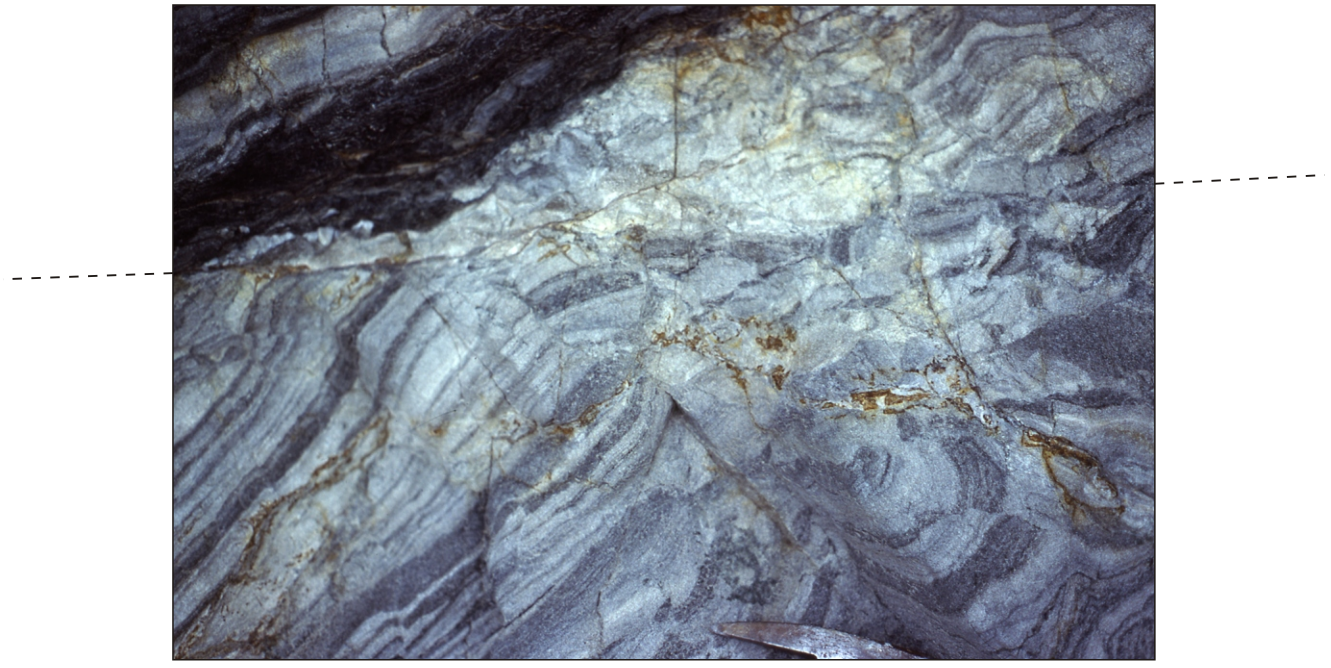

Plate 12

Plates 11, 12

Box folding as a result of conjugate kink development in the top left hand corner of Plate 11. Possible thrust fault as shown from lower left to upper right of Plate 11. Plate 12 is an enlargement of part of Plate 11 near the geology pick showing disrupted layering due to kinking and the possible thrust fault. Louisa Bay (447300/5181400).

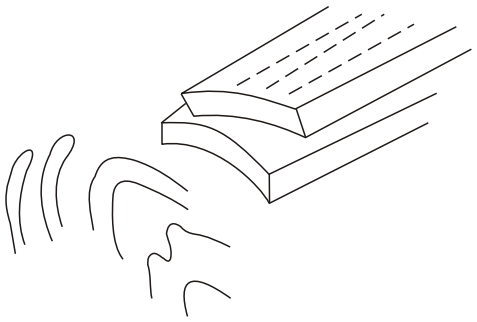

Figure 24

Mesoscopic recumbent folding in the white, well jointed and layered metaquartzite. The dashed line corresponds to the secondary foliation–layering intersection lineation. Red Point Hills (442800/5183800).

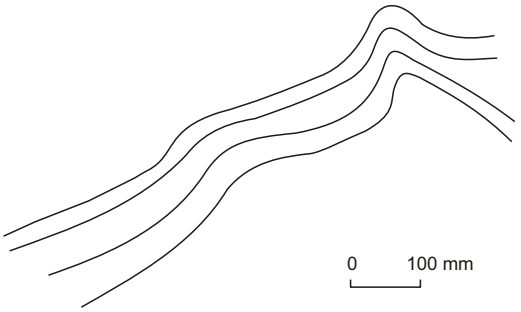

Figure 25

Folded, layered metaquartzite. The folds are monoclinal and close, asymmetric, gently plunging and upright. Ironbound Range (454300/5181100).

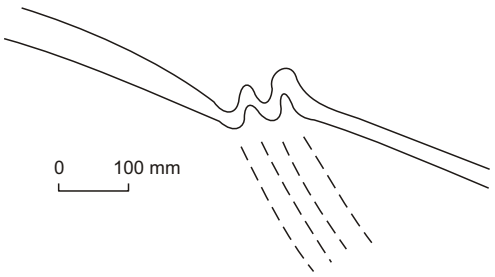

Figure 26

Tight mesoscopic chevron-like fold with steeply plunging hingeline. Red Point Hills.

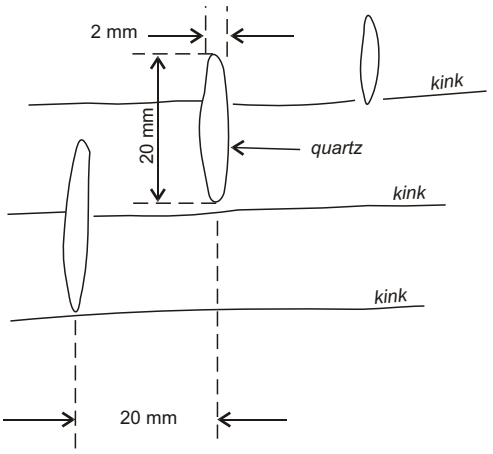

Figure 27

Wisps of quartz elongated parallel to the layering/foliation lineation within the pelitic sequence. There are numerous kinks cross cutting this lineation. Louisa Bay near Anchorage Cove (446300/5181100).

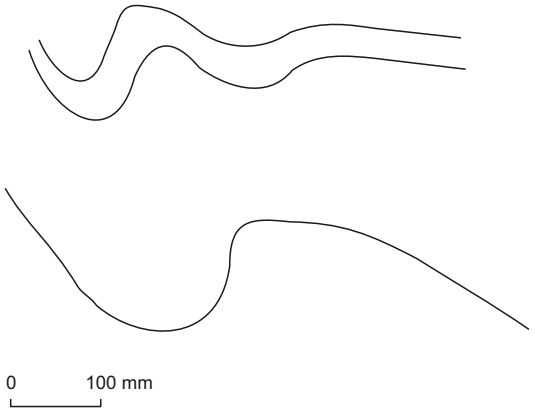

Figure 28

Mesoscopic folding in the well layered metaquartzite sequence showing the typical gently-plunging, upright asymmetric folds. Base of the Ironbound Range on the South Coast Track (453000/5184100).

Figure 29

Gently-plunging, upright asymmetric mesoscopic fold. Base of the Ironbound Range on the South Coast Track (453400/5183700).

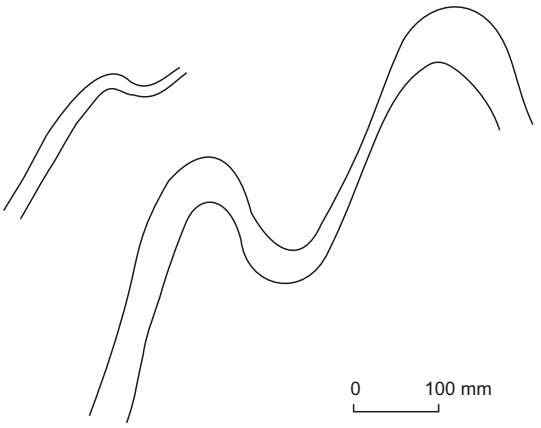

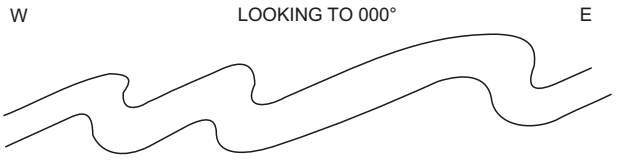

Figure 30

Mesoscopic asymmetric folding on the eastern limb of a minor antiform (half wavelength ~ 50 m). Louisa Bay foreshore cliffs near Louisa Creek (447300/5181400).

Figure 31

Black, ptygmatic-like folded layer within a light grey pelitic sequence. Louisa Bay (447600/5181400).

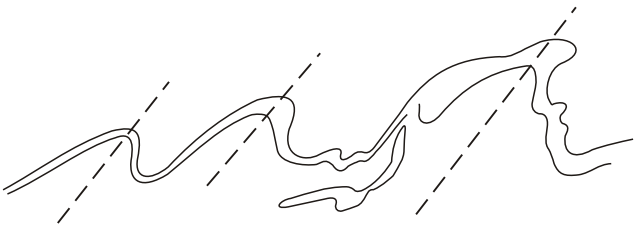

Summary and conclusions

The metamorphosed Precambrian sequence in the Louisa Creek area consists of a pelitic sequence with metaquartzite layers and a metaquartzite sequence. The metaquartzite is overlain by comparatively unmetamorphosed conglomerate, then a quartzite sequence near the top of the Ironbound Range.

The metamorphosed Precambrian rocks exhibit folded mechanical layering with an associated foliation (crenulation cleavage or differentiated crenulation cleavage) as well as later mesoscopic fold development and late-stage kinking. These major folds and the different sequences have also been faulted at a later stage.

References

HALL, W. D. M.; MCINTYRE, M. H.; HALL, K. 1969. *South-west Tasmania EL13/65. Geological report 1966–67.* Broken Hill Proprietary Company Limited Exploration Department [TCR69-0552].

POWELL, C. M. 1979. Timing of slaty cleavage during folding of Precambrian rocks, north-western Tasmania. *Bulletin Geological Society of America* 85:1043–1060.

WILLIAMS, P. R.; CORBETT, E. B. 1977. *Geological atlas 1:250 000 series. Sheet SK55/7. Port Davey*. Department of Mines, Tasmania.

WILLIAMS, P. R. 1979. *Basin development, environment of deposition and deposition of a Precambrian(?) conglomeratic flysch sequence at Bathurst Harbour, SW Tasmania*. Ph.D. thesis, University of Tasmania.

[27 August 2013]

APPENDIX 1

Locations of registered samples

Field Number	*Registered Number*	*AMG Co-ordinates*
BA1	1981-1	441 800 mE; 5 203 200 mN
BA2	1981-2	445 600 mE; 5 198 200 mN
BA3	1981-3	445 200 mE; 5 197 000 mN
BA4	1981-4	448 000 mE; 5 200 400 mN
BA5	1981-5	446 800 mE; 5 196 200 mN
BA6	1981-6	445 500 mE; 5 195 300 mN
BA7	1981-7	449 000 mE; 5 203 700 mN
BA8	1981-8	452 400 mE; 5 184 500 mN
BA9	1981-9	453 000 mE; 5 184 100 mN
BA11	1981-10	447 300 mE; 5 181 600 mN
BA12	1981-11	447 300 mE; 5 181 600 mN
BA13	1981-12	448 800 mE; 5 185 300 mN
BA15	1981-13	449 200 mE; 5 179 700 mN
BA16	1981-14	444 000 mE; 5 183 900 mN
BA17	1981-15	446 300 mE; 5 186 300 mN
BA19	1981-16	445 800 mE; 5 180 900 mN
BA20	1981-17	446 200 mE; 5 181 200 mN
BA22	1981-18	454 700 mE; 5 180 900 mN
BA23	1981-19	444 100 mE; 5 186 400 mN
BA24	1981-20	443 600 mE; 5 187 200 mN
BA25	1981-21	443 900 mE; 5 183 300 mN